APPROVED FOR PUBLIC RELEASE;
DISTRIBUTION IS UNLIMITED (A)

brimrose corporation of america • 7720 belair road • baltimore, maryland 21236
301/668-5800 • telex: 910-997-6817
• fax: 301-668-5977

DEVELOPMENT OF A DIGITAL X-RAY TOPOGRAPHIC MAPPING TECHNIQUE

FOR

AUTOMATED, RAPID CHARACTERIZATION OF PRODUCTION GaAs WAFERS

CLEARED
FOR OPEN PUBLICATION

JUN 2 1995

DIRECTORATE FOR FREEDOM OF INFORMATION
AND SECURITY REVIEW (OASD-PA)
DEPARTMENT OF DEFENSE

FINAL REPORT

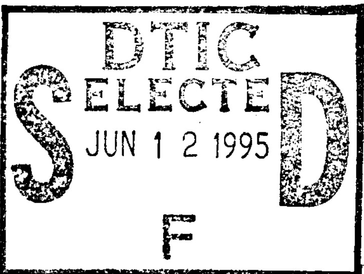

Sponsored by

Defense Advanced Research Projects Agency (DoD)

Defense Small Business Innovation Research Program

ARPA Order #5833

Issued by U.S. Army Missile Command Under

Contract #DAAH01-86-C-1047

REVIEW OF THIS MATERIAL DOES NOT IMPLY
DEPARTMENT OF DEFENSE INDORSEMENT OF
FACTUAL ACCURACY OR OPINION.

This document has been approved
for public release and sale; its
distribution is unlimited.

APPROVED FOR PUBLIC RELEASE;
DISTRIBUTION IS UNLIMITED (A)

TECHNICAL MONITOR:	Mr. Dempsey
NAME OF CONTRACTOR:	Brimrose Corporation of America
BUSINESS ADDRESS:	7720 Belair Road, Baltimore, MD 21236
PRINCIPAL INVESTIGATOR:	Dr. Ronald G. Rosemeier
CO-PRINCIPAL INVESTIGATOR:	T. S. Ananthanarayanan
INVESTIGATORS:	Dr. S. B. Trivedi Alfred L. Wiltrout Douglas C. Leepa
CONTRACT CONSULTANTS:	Dr. William E. Mayo Dr. Paul J. Coyne
EFFECTIVE DATE OF CONTRACT:	September 30, 1986
CONTRACT EXPIRATION DATE:	March 30, 1988
REPORTING PERIOD:	Final

19950607 065

REPORT DOCUMENTATION PAGE

Form Approved
OMB No. 0704-0188

Public reporting burden for the collection of information is estimated to average 1 hour per response, including the time for reviewing instructions, searching existing data sources, gathering and maintaining the data needed, and completing and reviewing the collection of information. Send comments regarding this burden estimate or any other aspect of this collection of information, including suggestions for reducing this burden, to Washington Headquarters Services, Directorate for Information Operations and Reports, 1215 Jefferson Davis Highway, Suite 1204, Arlington, VA 22202-4302, and to the Office of Management and Budget, Paperwork Reduction Project (0704-0188), Washington, DC 20503

1. AGENCY USE ONLY *(Leave blank,*

2. REPORT DATE
Mar 30, 1988

FINAL REPORT

4. TITLE AND SUBTITLE
DEVELOPMENT OF A DIGITAL X-RAY TOPOGRAPHIC MAPPING TECHNIQUE FOR AUTOMATED, RAPID CHARACTERIZATION OF PRODUCTION GaAs WAFERS

5. FUNDING NUMBERS

7. PERFORMING ORGANIZATION NAME(S) AND ADDRESS(ES)
BRIMROSE CORPORATION OF AMERICA
7720 BELAIR ROAD
BALTIMORE, MD 21236

8. PERFORMING ORGANIZATION REPORT NUMBER
DSRS U 33931

9. SPONSORING/MONITORING AGENCY NAME(S) AND ADDRESS(ES)
ADVANCE RESEARCH PROJECT AGENCY
3701 FAIRFAX DRIVE
ARLINGTON, VA 2203

10. SPONSORING/MONITORING AGENCY REPORT NUMBER
DAAH0186C1047

11. SUPPLEMENTARY NOTES

12a. DISTRIBUTION/AVAILABILITY STATEMENT
UNCLASSIFIED

12b. DISTRIBUTION CODE

13. ABSTRACT *(Maximum 200 words)*

THIS RESEARCH PROGRAM WAS TO DEVELOP A DIGITAL AND AUTOMATED X-RAY TOPOGRAPHIC TECHNIQUE FOR USE AS A RAPID QUALITY CONTROL TOOL IN CHARACTERIZING 3" GaAs WAFERS.

THE CONCLUSIONS SHOW THAT THE DARC TOPOGRAPHY SYSTEM IS A TOOL CAPABLE OF PROVIDING USERS WITH THE INFORMATION NEEDED TO CHARACTERIZE PRODUCTION III-V AND II-VI SEMICONDUCTOR WAFERS.

14. SUBJECT TERMS
WAFER
X-RAY
GaAs

15. NUMBER OF PAGES

16. PRICE CODE

17. SECURITY CLASSIFICATION OF REPORT	18. SECURITY CLASSIFICATION OF THIS PAGE	19. SECURITY CLASSIFICATION OF ABSTRACT	20. LIMITATION OF ABSTRACT
SAR			SAR

NSN 7540-01-280-5500

Standard Form 298 (Rev. 2-89)
Prescribed by ANSI Std. Z39-18

1.0 OBJECTIVE

The objective of this research program was to develop a digital and automated x-ray topographic technique for use as a rapid quality control tool in characterizing 3" GaAs wafers.

2.0 METHOD

Following the established viability in Phase I, the x-ray rocking curve analysis was the primary method followed in the pursuit of quantitative defect density mapping.

3.0 ADVANTAGE

The principle advantage of the x-ray rocking curve technique is that the method is non-invasive (non-contacting and non-destructive) in nature, and can be utilized for on-line production applications.

4.0 TECHNICAL-PROGRESS

To begin the program, numerous samples were acquired from various sources such as Army Night Vision Labs, Rockwell International, Bell Northern Research, DuPont, 3M, and Texas Instruments. These samples include a variety of substrates and epitaxial films, e.g. ZnSe/GaAs, PbSe/BaF_2, Si, $LiNbO_3$, GaP, Ge, SiO_2, ZnCdTe, HgMnTe, HgCdTe/CdTe, CdTe, and others. The purpose of collecting such a large spectrum of materials was to prove potential in many different applications.

The preliminary results from some of the afore-mentioned substrates and molecular beam epitaxial (MBE) films indicated the ability that the DARC (Digital Automated Rocking Curve) topography technique has for characterizing process induced micro-structural damage. By choosing the appropriate Bragg reflections for each individual sample and utilizing a two-dimensional (2D) detector, rocking curve half-width maps for an area of the wafer were obtained. The 2D dislocation density maps were then built from these half-width maps. With this information, the deconvolution of micro-plastic lattice strain from the total strain tensor is now possible.

In further studies, substrate and epitaxial layer lattice parameters and quality were measured utilizing the DARC system and compared with more conventional x-ray rocking curve techniques. The results were favorable; and can be found in the paper entitled "X-ray Analysis of Complex III-V Epitaxial Structures," see attached Appendix A.

A thermo-electrically cooled charge coupled device (CCD) was tested and integrated into the system. The spatial resolution of the camera is 20 to 30 microns. Unfortunately, because of the cameras large size and high price, it would be difficult to incorporate it into a commercial on-line quality control system. Therefore, while some research was still accomplished utilizing this detector, most work was done with the DIXIE (Digital Intensity X-ray Image Enhancer) detector.

New studies were developed to analyze surface and sub-surface damage due to various abrasive particle sizes used in the polishing process which all semiconductor wafers must undergo before being built on. The findings of this work were presented at the 14th International Symposium on Gallium Arsenide and Related Compounds.

The final study of the program was on wafers with devices built on them. Strain fields created by the electrode mountings on quartz oscillators were analyzed along with those caused by 1 K RAM devices built on GaAs.

5.0 SYSTEM-PROGRESS

Over the course of the contract, the DARC topography system was continually upgraded and improved. Major advances were made in the software controlling system and in the motors and stages used to physically manipulate the wafers. The resultant system was controlled by four stages with high resolution motors. The rocking axis was controllable to 0.36 arc seconds. The four stages included: rotation of incidence angle, rotation of azimuthal angle, linear depth alignment, and linear sample displacement from the source. All motors are software controllable and include local lock-out when the experiment is in progress.

The software has four basic sections: analysis parameter collection, image acquisition, data analysis, and image display.

1) Analysis-Parameters: Parameters are collected by accessing a form window which allows the user to adjust any parameters as necessary. When all of the entered data is correct, the window can be exited to save the new data or even be terminated so as to erase all of the changes and continue with the original configuration.

2) Image-Acquisition: This section of the software allows the user to choose a window with 'x' by 'y' dimensions from the following choices: 10,20,40,80 pixels long on either axis. The selected window can then be interactively located anywhere on the image plane (512 x 481 pixels) through the use of simple keyboard commands.

3) Data-Analysis: The data analysis section computes the Bragg peak shift (elastic strain), Bragg peak broadening (plastic strain/dislocation density), and Bragg peak integrated intensity for each pixel in the 'x' by 'y' pixel window. Pseudo-color is used to depict these measurements for each pixel.

4) Image-Display: The computations from section 3 are then displayed as a two-dimensional map with pseudo-color. This section also allows the user to display the x-ray intensity profile of any and every pixel in the window as a function of the rocking angle. The user can then utilize these rocking curve profiles to determine lattice parameter mismatch and associated micro-lattice strains in the material under examination.

At this point, the user is able to return the image acquisition window and the sample to the same position from which they were initiated at the start of the just finished run. This allows for full wafer mapping of wafers up to 35 millimeters in diameter to be accomplished by running the rocking curve experiment a number of times; and moving the image acquisition window to a new position each time the experiment runs until

the entire wafer has been mapped. Each time the user runs the rocking curve, they are given the option of storing the specific window's Bragg Peak Shift, Bragg Peak Broadening, and/or Integrated Intensity displays. Once all desired window displays have been saved, the user can then start displaying the full wafer map. Each window can be recalled and replaced in its original position. Once the entire wafer is displayed, the user has the option of performing a histogram equalization on a selected area of the wafer. Performing the equalization expands the map of the selected area over the full 128 gray level (or pseudo-color) range, thereby unmasking possible hidden data.

The system was also hooked to a Tektronix color ink jet printer. At any time while using the DARC system, it was possible to get a hard-copy of the image processor output. Numerous prints have been enclosed in Appendix B that show the various types of data and materials that were used.

6.0 CONCLUSIONS

As was made obvious in the Technical-Progress and System-Progress sections, many papers that discuss in detail the results found during this contract were presented at various conferences and published in the proceedings of several symposiums where the pursuit of quality semiconductor materials was of major concern. Instead of rewriting these papers for this report, they have been included in their original forms.

The conclusions drawn in these papers certainly do show that the DARC topography system is a tool capable of providing users with the information needed to characterize production III-V and II-VI semiconductor wafers.

Accesion For
NTIS CRA&I ☑
DTIC TAB ☐
Unannounced ☐
Justification
By
Distribution /
Availability Codes
Dist | Avail and / or Special
A-1

brimrose

APPENDIX A

X-ray Analysis of Complex III-V Epitaxial Structure

T. S. Ananthanarayanan and D. C. Leepa

Brimrose Corporation of America, 7720 Belair Road, Baltimore, MD 21236

AlGaAs/GaAs (HEMT) Epitaxial Film (MBE)

Figure 1 shows the morphology of the complex heteroepitaxial structure used here to illustrate the effectiveness of the x-ray rocking curve topography for measuring microstructural features. The x-ray beam used for this work was unmonochromated Cu K_α radiation as discussed previously. Several reflections were examined for this specimen. By changing the Bragg reflection analyzed, the interrogation depth can be varied from 2-20μm.

However, the alignment of the apparatus for such measurements is extremely critical. Figure 2 shows the rocking curve profile along a vertical cursor line (10 profiles superimposed on one another) in the 10 x 10 pixel window area. This window corresponded to 1 mm x 1 mm sampling area. Surface orientation of this specimen was determined to be (001) by back reflection Laue. The (422) and the (311) rocking curves exhibit two pairs of maxima corresponding to $K_{\alpha 1}$ & $K_{\alpha 2}$ of epi (AlGaAs) and substrate (GaAs). From the close proximity of these peaks it is quite evident that the lattice matching is very high in this specimen. Contrast these results with the next specimen.

InGaAs/InP Heteroepi Film (MOCVD)

This specimen is illustrated to show poorly matched structure in comparison to the sample in 3.1. The various rocking curve profiles shows the $K_{\alpha 1}$ and $K_{\alpha 2}$ pairs for InGaAs epi and InP substrate. The rocking curve profiles of this sample from various hkl's appear significantly different indicating the effect of interrogation depth. At this juncture it should also be noted that information at varying depths can be obtained by:

1) changing hkl reflection, and
2) changing incoming x-ray wavelength (and hence penetration depth).

The results presented here are a comparison between the well known DCD (double crystal diffractometer) rocking curve measurements and the white beam (unmonochromated) x-ray rocking curve measurements. The specimen examined was a complex hetero-epitaxial InGaAs/InP. The details of the structure can be seen in Figure 3a. Figure 3b illustrates typical DCD (004) rocking curve from this sample. From Table 1 the penetration depth of the x-ray is 8.0μm for InP and 15.5μm for GaAs (about the same for InGaAs). It is therefore clear that the most intensity would come from the InP in the structure. Figure 4 shows the specimen and the points (approximately) at which the DCD rocking curves shown in Figure 5 were obtained. The trend in lattice mismatch can be observed by the displacement between the InP and the InGaAs peaks. Figure 6 shows a similar map done, using the Brimrose DARC topography system. The window size chosen was

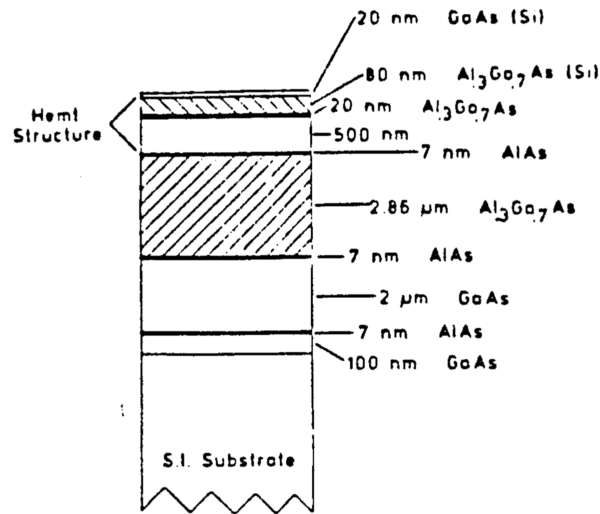

FIGURE 1 Morphology of Complex AlGaAs/GaAs HEMT Structure.

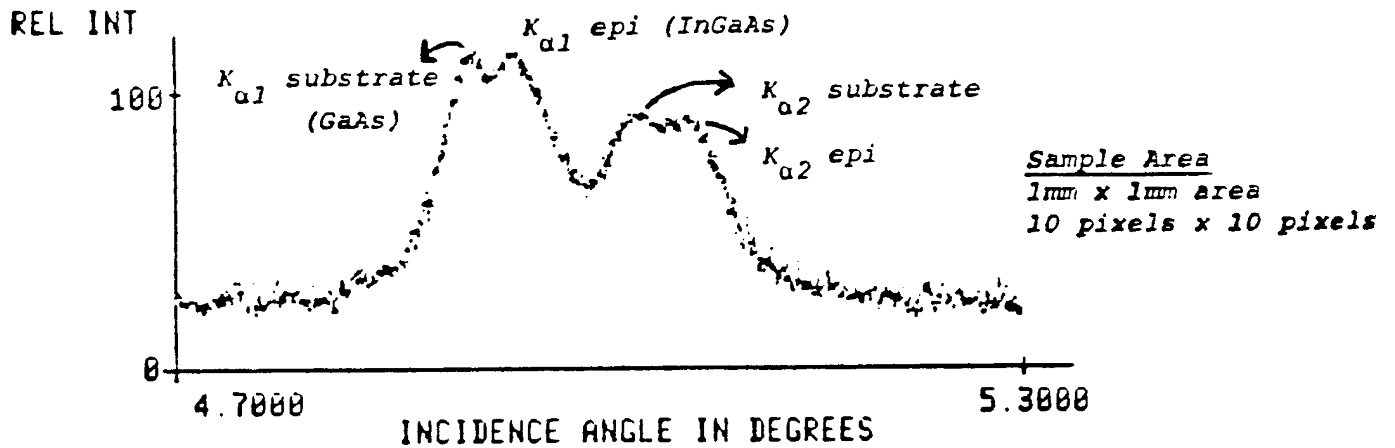

FIGURE 2 X-ray Rocking Curve Profile of AlGaAs/GaAs HEMT Structure Unmonochromated Cu K_{α} Radiation.

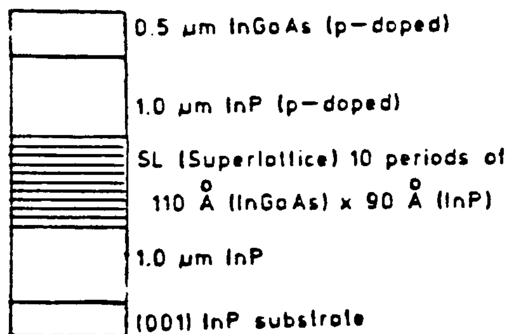

FIGURE 3a Details of InGaAs/InP Heteroepitaxial Structure

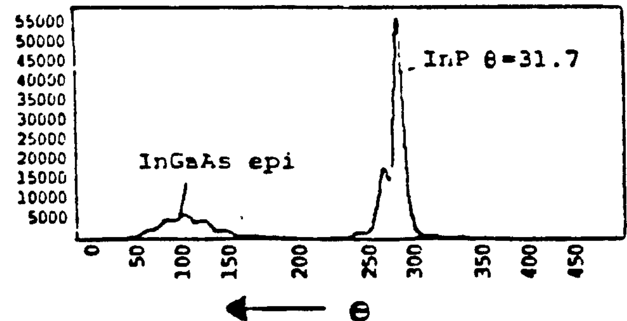

FIGURE 3b Typical DCD (004) Rocking Curve of Sample in 5a.

FIGURE 4 Double Crystal Rocking Curve Map Points on InGaAsP/InP Complex Heteroepitaxial Sample.

FIGURE 5 DCD Rocking Curve Map Showing Mismatch at Various Locations on Sample Points in Figure 4.

INCIDENT X-RAY BEAM UNMONOCHROMATED Cu K_α RADIATION
InGaAs EPI/InP SUBSTRATE

FIGURE 6 DARC Rocking Curve Profiles. Contrast with Figure 5.

100 x 100 pixels (1 x 1 mm). Data shown is an entire column (vertical) of 10 pixels superimposed on one another (hence, the slight scatter). However, the trend in mismatched is identical to that seen in Figure 7. The rocking curve profiles shown in Figure 8 are from the (422) reflection. From Table 1 the penetration depth in InP is 2.3μm and is 5.9μm in GaAs. The intensity of the epi and the substrate are comparable in profile in Figure 8, four distinct peaks can be observed at this map point[1]. These are the $K_{\alpha 1}$, and $K_{\alpha 2}$ of substrate and $K_{\alpha 1}$ $K_{\alpha 2}$ of epi film respectively from left to right . This case represents the worse case of lattice mismatch. As the degree of mismatch decreases the epi peaks migrate towards the substrate peaks and for ideal lattice matching will be superimposed on the substrate peaks (there will be only 2 peaks in all). The angular differences shown in Figure 6 are between $K_{\alpha 1}$ substrate and $K_{\alpha 2}$ epi. This is so only because of convenience in peak position determination of these two peaks in all profiles shown. Other structures with less mismatch are now being examined e.g., AlGaAs epi/GaAs substrate. Figure 7 shows the (335) reflection. This reflection from Table 1 shows a penetration depth of 0.5μm. Therefore, the signal observed in Figure 4 can be attributed predominantly to the final InGaAs 0.5μm layer (hence only two peaks $K_{\alpha 1}$, $K_{\alpha 2}$ of epi InGaAs). It is quite evident that by changing the (hkl) at the detector end (hence, varying depths of penetration) various layers in the heteroepi structure can be interrogated. Also it is possible to compile the strain tensor in the material under investigation.

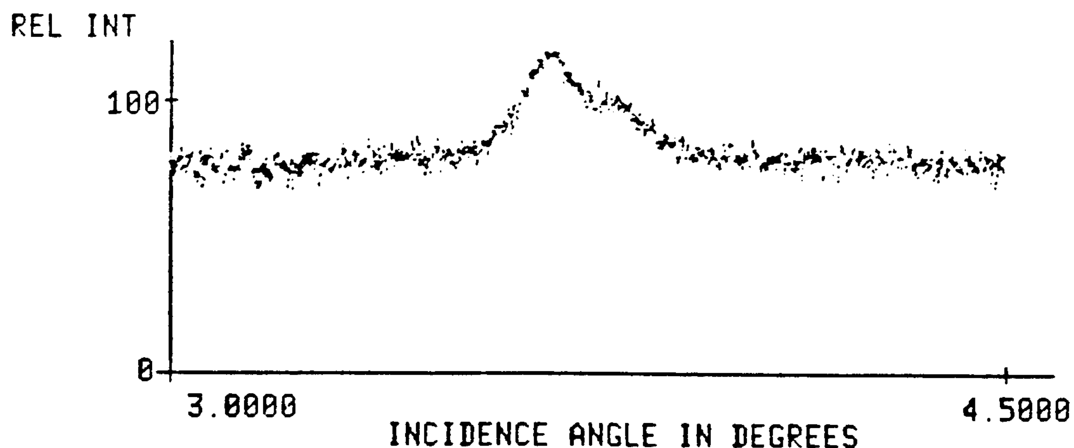

FIGURE 7 (335) Rocking Curve Profile of InGaAs/InP Heteroepitaxial Structure.

TABLE 1

Diffraction Data for Reflection Topography of (100) Surface Using Cu K_α Radiation.

Reflecting Planes	Inclination to Surface (ϕ) (100) Surface	Gallium Arsenide $u = 404\ cm^{-1}$ $\gamma = 0.31$			Indium Phosphide $u = 760\ cm^{-1}$ $\gamma = 0.36$		
		θ (deg)	Δθ (sec)	t (um)	θ (deg)	Δθ (sec)	t (um)
311	25.3	26.9	39.4	1.5	25.8	72.2	0.3
400	0	33.0	8.3	15.5	31.7	7.8	8.0
422	35.3	41.9	20.0	5.9	40.0	21.8	2.3
511	15.8	45.1	6.2	17.9	43.0	6.9	9.0
440	45	50.4	20.4	4.9	48.0	25.6	1.5
531	32.3	53.7	7.3	15.2	51.0	8.3	7.3
620	18.5	59.5	7.9	22.4	56.1	7.3	11.3
533	40.3	63.3	7.6	15.9	59.4	8.6	7.4
335	62.8	63.3	45.7	0.5	< θ		
444	54.8	>70			65.4	14.5	4.6

M A G Halliwell, J B Childs and S O'Hara

MICROLATTICE STRAIN MEASUREMENTS ON QUARTZ OSCILLATORS

Two distinct oscillator types have been evaluated for contrasting microlattice strain fields developed due to electrode bonding:

a. lateral field excitation mode crystal and
b. transverse field excitation mode crystal.

Lateral Field Excitation Crystal (Two Point Mount)

The operating frequency of this oscillator (shown in Figure 8) was 5 MHz. Its $Q = 5 \times 10^5$ and the quality of quartz used was not the best. The electrode bonding was on the top and bottom surface of the oscillator crystal (two point mount) which was a few mils thick. Figure 9 shows the reflection x-ray rocking curve topograph of the lateral field oscillator. The information contained in this reflection topograph is predominantly from the surface (< 7μm) of the oscillator crystal. Figure 10 shows the transmission x-ray rocking curve topograph of this oscillator crystal. Both Figure 9 and 10 clearly indicate the contours of the microlattice strain state in the oscillator crystal. The pattern of the strain field seem to strongly indicate that the solder and the mechanical contacts made for electrodes as being the origin of the strain field.

Transverse Field Excitation Crystal (Three Point Mount)

This mounting mode for the oscillator crystal is inherently less vibration sensitive. This oscillator was a high precision space qualified resonator made of high purity Z-growth quartz (low Al impurity content) with 5 MHz operating frequency. Its microwave $Q = 2.5 \times 10^6$. Due to low Al impurity content this resonator has low radiation sensitivity. For high performance oscillators:

typical microwave $Q = 2.5 \times 10^6$

frequency stability $f = 2 \times 10^{-9}$/day or better

temperature dependance of $f < 10^{-6}$/c

radiation sensitivity $< 1 \times 10^{-10}$/radiation

Figure 11 depicts the high precision oscillator used in this study, with and without the glass vacuum encapsulant. Figure 12 and Figure 13 are two different (hkl) reflection Berg-Barrett x-ray topographs obtained at different Bragg angles (53° and 65° respectively) Figure 12 shows the gold electrode masking the central area of the oscillator crystal while Figure 13 shows information coming through the gold electrode (showing $K_{\alpha 1}$ and $K_{\alpha 2}$ reflections). This is due to the fact that the (hkl) reflection used in Figure 13 has a much higher penetration depth (> 500 A) in comparison to that in Figure 12 (< 500 A). Therefore, if is evident that by varying Bragg plane for topography (hkl), the interrogation depth can be routinely changed.

Figure 14 shows the DARC rocking curve topograph of the (hkl) Bragg reflection in Figure 13. The strain field is not as pronounced as in the lateral field oscillator (section 2.1 Figures 9 and 10). It should be noted at this point that the mounting of the crystals in two cases was different (two point and three point). The electrodes in Figure 8 were mounted on the top and bottom surfaces of the crystal. Where as in Figure 11, the 3 electrodes were mounted on the sides of the crystal. Additionally, the thickness of the transverse mode crystal was about 1mm in comparison with lateral field crystal which was only a few mils. Figure 14 shows typical growth striations (dislocations) and a slight deviation at the points where the electrode was attached (N-E Quadrant).

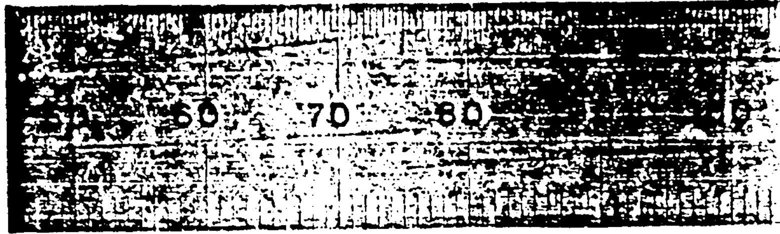

TOP VIEW

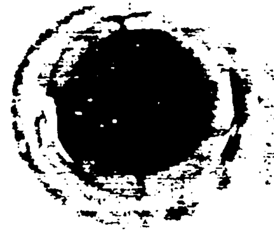

SIDE VIEW

SIDE VIEW
WITH
GLASS ENCAPSULANT

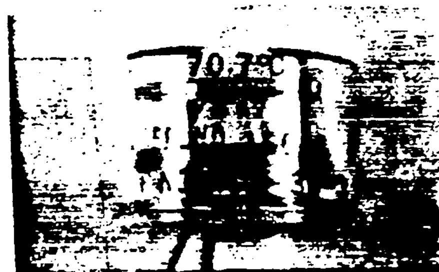

FIGURE 11 Transverse Field Excitation Crystal With and Without Glass Encapsulant.

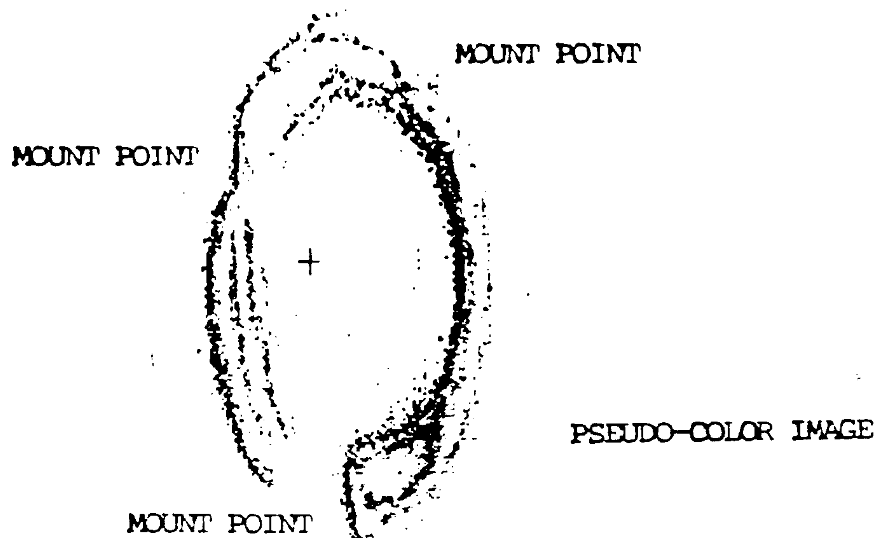

FIGURE 12 Berg-Barrett Reflection Topograph of Transverse Field Oscillator Crystal. Center of Image Blocked by 500 A Gold Electrode. Vertical Image Distortion Due to Vertical Divergence in X-ray Topography System. Bragg Angle = 53 deg. Incidence Angle = 0.6 deg.

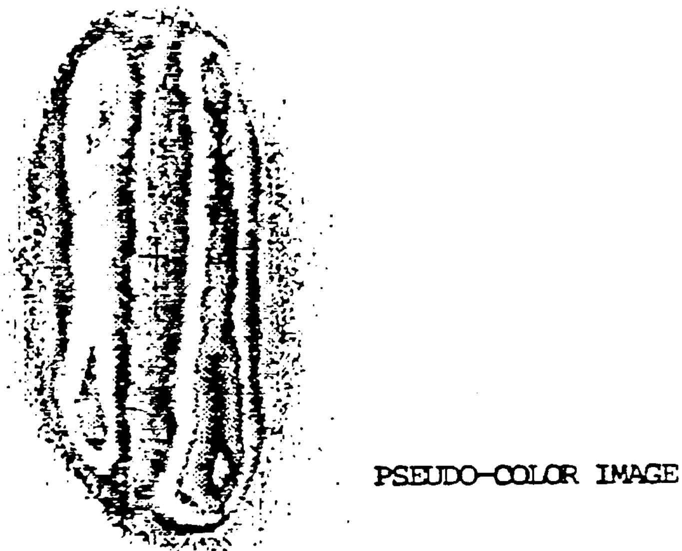

FIGURE 13 Berg-Barrett Reflection Topograph of Transverse Field Oscillator Crystal. Penetration Depth far Below Gold Electrode. $K_{\alpha 1}$ and $K_{\alpha 2}$ Reflections Seen from Quartz Substrate. Bragg Angle = 65 deg. Incidence Angle = 3.7 deg.

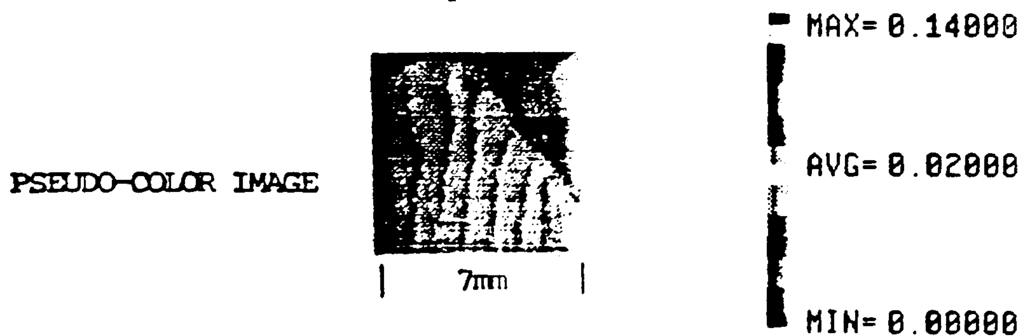

FIGURE 14 Rocking Curve Topograph (Half Width Map) of Reflection in FIGURE 12. Growth Striations Distorted at Mounting Point.

Paper Presented at the DRIP II International Symposium on

Defect Recognition and Image Processing in III—V Compounds

Monterey, California

DARC*, A NOVEL TOPOGRAPHIC TECHNIQUE FOR RAPID NON-DESTRUCTIVE CHARACTERIZATION OF III-V COMPOUNDS

T. S. ANANTHANARAYANAN and S. B. TRIVEDI

Brimrose Corp. of America, 7720 Belair Road, Baltimore, MD 21236

SUMMARY

III-V compounds, both epitaxial and bulk, have become very important in the development of high speed devices. The performance of these devices is critically dependent upon the micro-structural integrity of the materials. The current study focuses on a recently developed novel X-ray diffraction technique which allows quantitative, near-real time topographic mapping of crystalline micro-lattice strains. The technique achronymed DARC (Digital Automated Rocking Curve) topography is essentially non-destructive, non-intrusive and non-contacting in nature.

DARC topography has been successfully used to characterize surface and sub-surface micro-lattice strains in various III-V materials including GaAs, AlGaAs, InP, InGaAs. Unlike conventional X-ray topographic techniques the DARC technique allows quantification and deconvolution of strain fields due to change in lattice parameter and variation in dislocation density. Using 2-D array X-ray detectors the analysis time has been dramatically reduced. Spatial resolution of this technique is currently 100um and can be improved to 20um using CCD X-ray detectors. Areas of the order of 1 $inch^2$ can be analyzed simultaneously (in 5 seconds). The sample size limitation can be overcome by increasing the incident X-ray beam size.

It is anticipated that the use of this system for online characterization of materials would result in significantly greater device yield, performance and reliability. Additionally, it will provide an extremely powerful analytical tool to quantify process induced microstructural changes.

INTRODUCTION

III-V based semiconductor materials are gaining significant stature in contrast to silicon due to their superior electronic and optical properties. Despite the maturity of silicon technology, materials' property limitation introduce constraints on device performance. GaAs is one III-V compound that is in the forefront of the high speed, high performance devices for military and civil applications. High carrier mobility hence high device speeds, high radiation tolerance, superior power capability and high temperature operation combine to give the III-V family of materials a distinct advantage over silicon. Some application areas for III-V compounds include ultra-high speed computers,

* DARC - Digital Automated Rocking Curve

high efficiency solar cells, microwave radar, television and satellite communications. In all of these applications, the performance and reliability of devices is critically dependent upon the microstructural integrity of the material.

In the past three decades, several techniques have been developed and utilized to study materials' microstructure and their electronic/optical properties. Some of these techniques include x-ray topography, electron microscopy, photoluminescence spectroscopy, photo-reflectance spectroscopy, cathodo-luminescence, etc. The objective of measurements made with these techniques is to establish a clear correlation between materials' microstructure and properties and hence predict device performance.

The present study focuses on a recently developed non-destructive, non-contacting x-ray technique to monitor material microstructure. This technique called DARC (Digital Automated Rocking Curve) topography[1] combines x-ray rocking curve analysis[2] with real-time diffraction topography[3]. Several investigations[4,5] in the past have utilized this technique to successfully study the subsurface microstructural morphology of numerous materials.

ROCKING CURVE TOPOGRAPHY

Rocking curve analysis is implemented in the DARC system by digitizing individual topographs through the image acquisition/processing hardware depicted in Figure 1. The technique utilizes the Berg-Barrett experimental geometry to obtain X-ray diffraction topographs. Figure 2 depicts X-ray optics involved. Specific (hkl) reflections can be observed by choosing the appropriate geometry. The surface orientation is obtained by conventional Laue back-reflection method.

Reflection topogr[illegible]hs obtained with the Berg-Barrett geometry are registered on a real time X-ray image intensifier[6]. This image is transfered to a video imaging system and then digitized by a video frame grabber[7]. The frame grabbing (30 frames/sec) is done with 7 bit resolution (128 gray levels) on a micro-computer based system. A detailed description of the experimental setup will be presented in a later section. Several images at incremental angles of incidence are digitized and stored for subsequent analysis. As seen in Figure

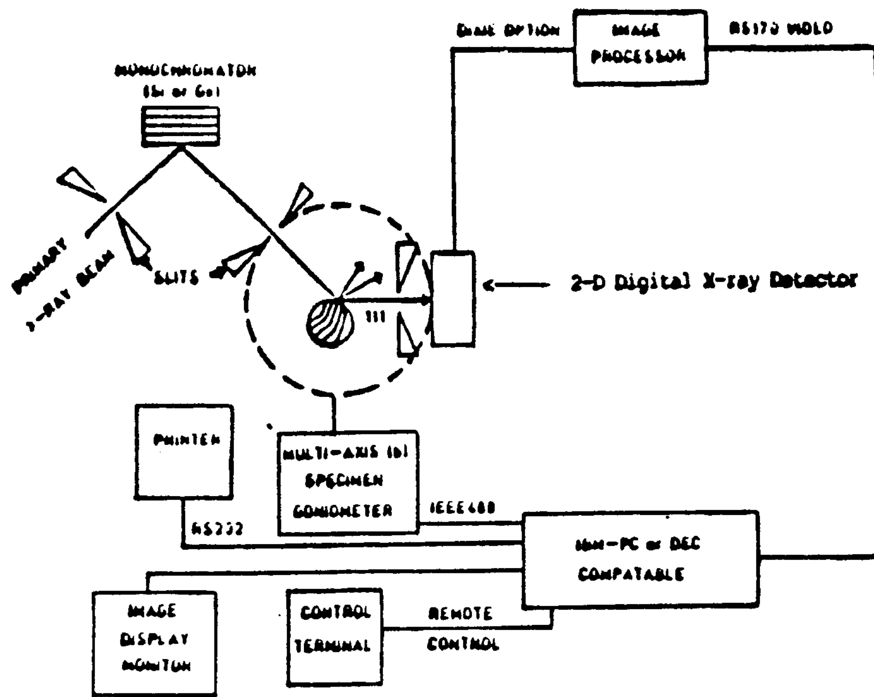

Figure 1 Schematic of Rocking Curve Analyzer

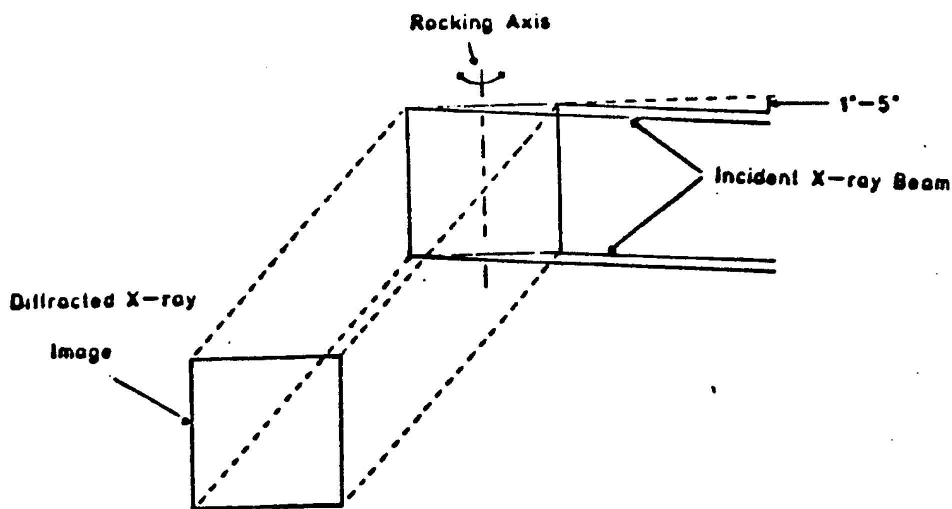

Figure 2 Diffraction Geometry for White Beam Rocking Curve Topography

2 the specimen surface is placed at a grazing angle of incidence (0.1 - 5.0 deg.). This provides an expanded area of incidence on the sample by a narrow beam of X-rays(line source). Thus resulting in a Berg-Barrett reflection at the appropriate "2-theta" position of the imager. The imager typically has a 40mm diameter window at 100um spatial resolution. The diffraction condition can be altered using a multi-axis computer controlled goniometer. One critical condition that is sought for rocking curve experiments is a "non-skew" reflection. This implies that the (hkl) plane under observation be parallel to the rocking axis or diffractometric axis. The diffractometric axis in this setup was aligned parallel to the incident beam(vertical). The diffractometer plane (normal to the rocking axis) was in this case represented by the horizontal plane. In order to ensure non-skew reflection the asimuthal orientation of the specimen had to be adjusted until the resulting reflection traversed along the diffractometer plane(equitorial/horizontal) when the specimen was rocked about the diffractometer axis. The diffractometer axis is defined by a precisely machined knife edge mounted about the specimen manipulator. The specimen is positioned to contain this diffractometer axis on its surface. The diffractometer axis is then positioned to bisect the incident beam. The alignment procedure enumerated above is critical for precise rocking curve measurements.

Rocking curve topography involves the combination of rocking curve analysis and diffraction topography. The diffracting domain of a given crystal is measured for a set of geometric conditions and X-ray beam optics. The diffracting domain of the crystal is a measure of the reciprocal volume of the crystal. The reciprocal volume is in turn related to the micro-lattice structure of the crystal. In general (kinematic theory) the reciprocal volume is inversely related to crystal perfection[8] i.e., as the amount of defects(imperfection) increase the reciprocal volume(diffracting domain) increases. However, for special cases such as thin epitaxial films the above generalization may not hold. It will be necessary to invoke the dynamic theory of X-ray diffraction[9] in such cases. The measurement will still be appropriate but the analysis will

be different. The current study uses the kinematic approach for the analysis. These substrates were prepared to minimize the effect of surface geometry on the rocking curve measurements. They were ground, polished and lapped minimal surface curvature.

Hardware Description

The x-ray optics and dimensions involved in the DARC imager are shown in Figure 2. The incident beam is typically a narrow line source and impinges on the specimen surface at a shallow incidence angle (1 - 5°). The 2-D digital x-ray detector shown in Figure 1 has an input window of 40mm diameter and can be positioned anywhere on the diffractometer circle. This position is a function of the diffraction vectors which in turn depend on the incident x-ray wavelength and lattice parameter of the specimen. Typically the incident x-ray wavelength can be anywhere between (0.5 - 5 Angstroms). Depending on the x-ray source, the upper and lower limits of the wavelength can be exceeded. The x-ray wavelength used in this system was an average of 1.54178 Angstroms ($\pm$ 0.005 Angstroms) which include $K_{\alpha 1}$ and $K_{\alpha 2}$ Cu radiation. The diffracted image is recorded by the 2-D detector. This image is then digitized and stored in the computer memory through an image processor. The specimen is rocked through its entire diffraction domain with the 2-D detector recorder at any desired resolution. The resolution can be controlled by varying the rocking speed (angular velocity) of specimen and the time between frame grabs in the image processor. Figure 1 depicts the schematics of the x-ray image detection and manipulation hardware. The goniometer (manipulator) is typically equiped with 6 degrees of freedom. The translation resolution is 0.1um and the rotation resolution is 0.1 arc sec. These are controlled by piezo-electric translators and optical encoders for precision. A prototype of the DARC imager is depicted in Figure 3.

Software Design

1. Grab Image
2. Store in memory, rotate specimen

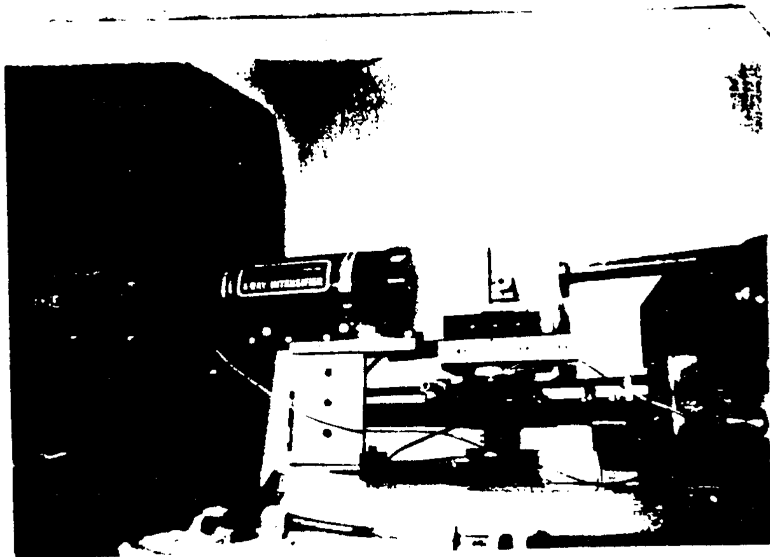

Figure 3a Side view of the DARC Imager.

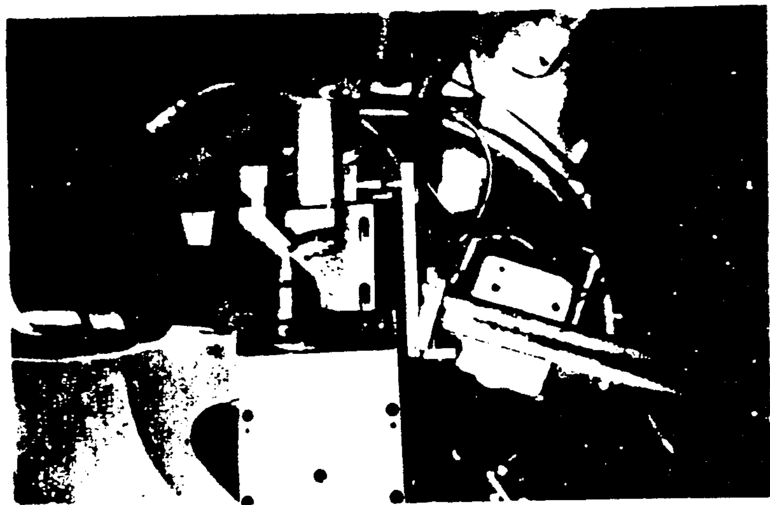

Figure 3b Top view of the DARC Imager.

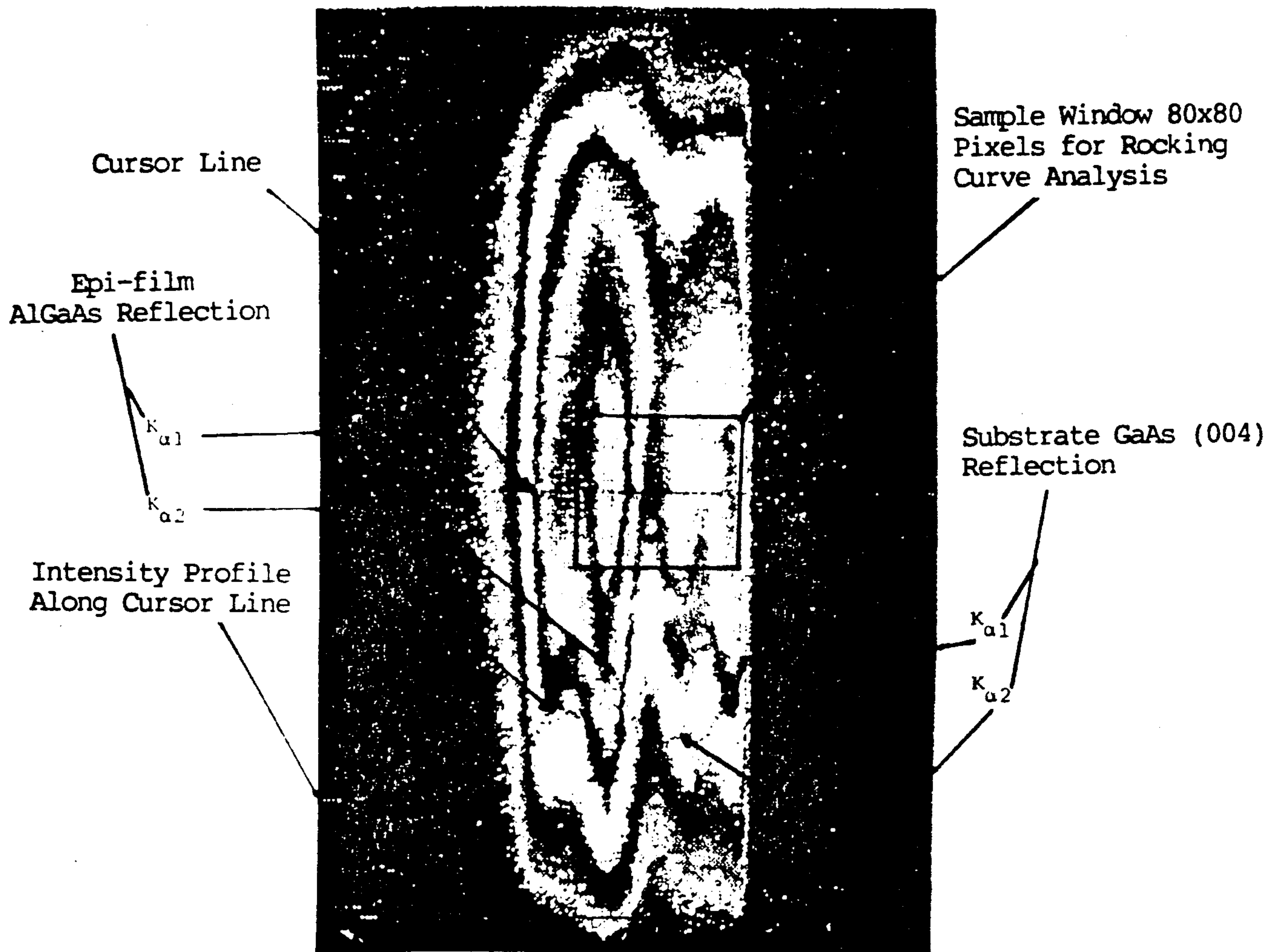

Figure 4 (004) Reflection Topograph from AlGaAs/GaAs Showing $K_{\alpha 1}$, $K_{\alpha 2}$ Reflections of Both Epi and Substrate. Pseudo Color Image.

3. Repeat steps 1 & 2 to cover entire diffracting domain with sufficient tail on either side of the reciprocal spot.

4. Compute θ_B (Bragg peak position), B (Bragg peak broadening) and I, Integrated Intensity (area under diffraction profile) for each pixel in the field of view.

5. Display θ_B, β & I as a function of topography.

   θ_B Map - Bragg peak position map

   β Map - Rocking Curve Halfwidth (FWHM) map. FWHM - Full Width at Half Maximum.

   I - Integrated Intensity Map - in case of epitaxial films, provides the film thickness as a function of topography.

DARC Imager Data Display Scheme

The critical feature in the display of the enormous volume of data generated by the DARC Imager is the use of pseudo-color to depict the 3rd dimension. In this case the 3rd dimension was the x-ray intensity and the reciprocal space parameters. The pseudo-color maps provide an easy to interpret and discern contour maps of the micro-lattice inhomogenietics present in various crystalline materials.

RESULTS AND DISCUSSIONS

Figure 4 depicts the (004) reflection from the AlGaAs/GaAs specimen. The reflection topograph was obtained from an unmonochromated Cu K incident radiation. Pseudo-color was used to accentuated the intensity contouring in the image. The intensity profile obtained along the cursor line is indicative of the color scale correspondence with actual x-ray intensity.

Figure 5 is the entire rocking curve experiment performed on the 80x80 pixels window shown in Figure 4. As the specimen is rocked incrementally about the rocking axis the reflection topograph goes through maxima at each pixel. In this case, it would be expected that each pixel would havefour maxima corresponding to $K_{\alpha 1}$, $K_{\alpha 2}$ reflections of both epi and substrate. Figure 6 shows the analysis results from the 80x80 pixel rocking curve experiment along the horizontal axis. Bragg peak broadening maps shows band structure of halfwidth (small magnitude of variation) possibly due to growth striation that is typical

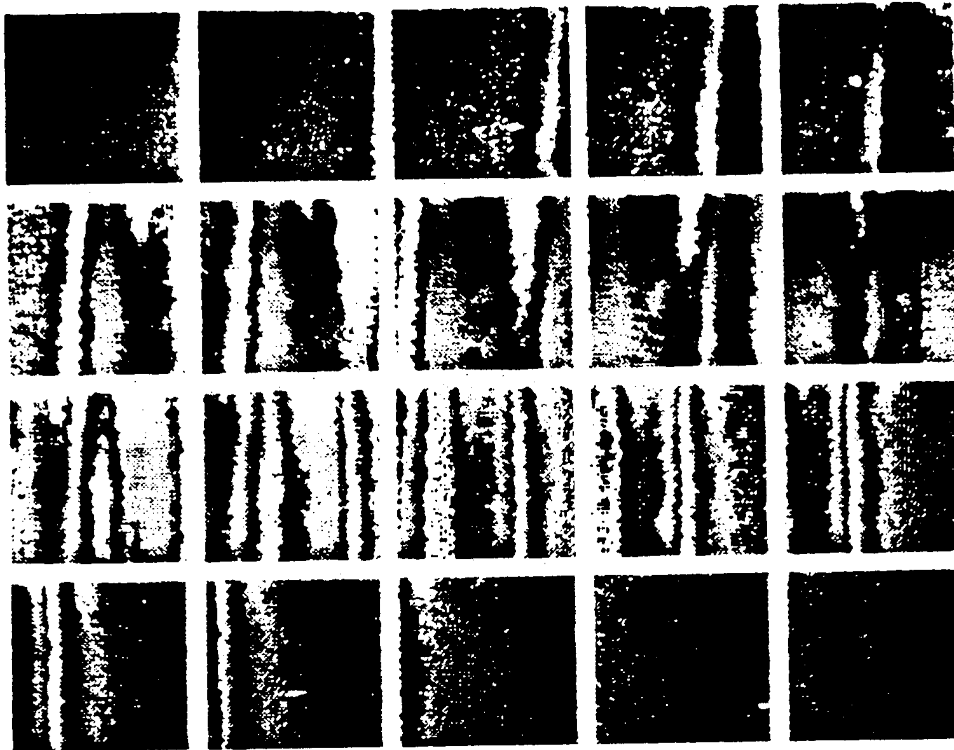

Figure 5 Rocking Curve Experiment on AlGaAs/GaAs Specimen, (004) Reflection. Angular Increment from Left to Right and Top to Bottom.

BRAGG-PEAK-SHIFT

MAX= 30.180 DEG

AVG= 30.1350 DEG

MIN= 30.0000 DEG

BRAGG-PEAK-BROADENING

MAX= 0.06600

AVG= 0.06000

MIN= 6.00005

INTEGRATED-INTENSITY

MAX= 61.0000

AVG= 52.0000

MIN= 4.0000

Figure 6 Rocking Curve Analysis of 80x80

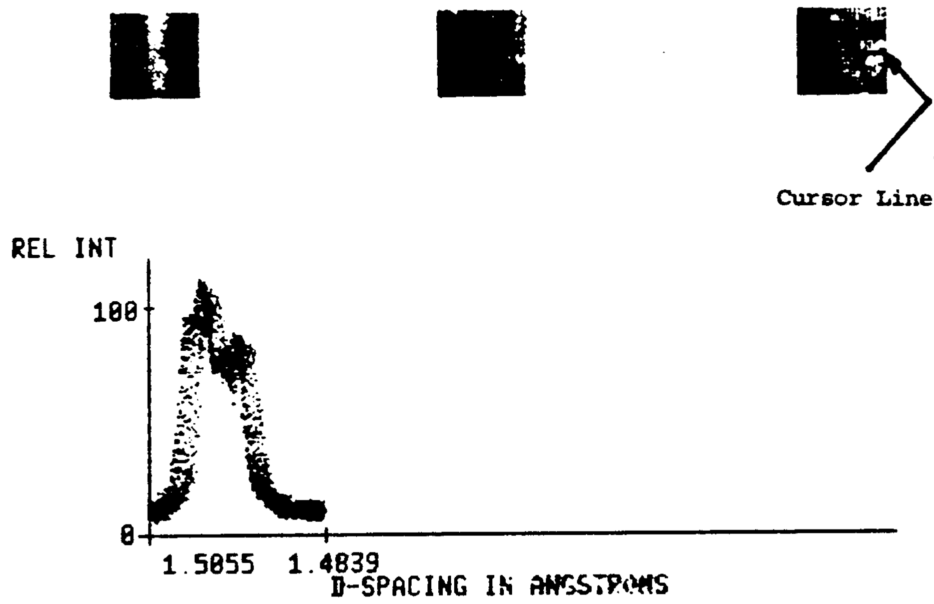

Figure 7 Rocking Curve Profiles along Indicated Cursor Line Peak Shift indicates Elastic Strain in Material.

in such materials. It is worthwhile to note at this point that the rocking curve analysis was performed only on the $K_{\alpha1}$, peak of GaAs for simplicity. However, in practice, each of the resolvable peaks can be used of the analysis. Use of the double crystal diffractometer with incident beam monochromation will greatly enhance resolution in the rocking curve analysis. The present study, used a conventional x-ray generator and was limited by the reduced x-ray beam intensity caused by monochromation. On the other hand, this limitation can be overcome by utilizing a high power x-ray source (rotating anode). Figure 7 shows the rocking curve results from a 40x40 pixels sample window. This figure also depices the rocking curve profiles for individual pixels along the cursor line indicated. Shift in Bragg peaks for each pixel is indicative of elastic strain in material along the horizontal axis.

CONCLUSIONS

Rocking Curve topography has been used to successfully study III-V compound semiconductors. The resolution of the technique needs to be improved. This can be accomplished by utilizing a high intensity x-ray source and a highly monochromated incident x-ray beam. 2-D rocking curve topography offers a rapid tool for quantifying subsurface microstructure in III-V compound semiconductors.

ACKNOWLEDGEMENTS

To Kathy A. Aversa and Dawn A. Roche for manuscript preparation. To Alfred L. Wiltrout, Douglas C. Leepa and Paul J. Coyne for data collection and analysis.

This reasearch was sponsored under contract #DAAH01-86-C-1047.

REFERENCES

1. T. S. Ananthanarayanan, R. G. Rosemeier, W. E. Mayo and S. Sacks, "Novel Nondestructive X-ray Technique for Near-Real Time Defect Mapping," 2nd Int. Symp. on the Nondestructive Characterization of Materials, Montreal, Canada, (July, 1986).

2. W. E. Mayo, R. Yazici, T. Takemoto and S. Weissmann, XII Congress of Int. Union of Crystallography, Ottawa, Canada (1981).

3. R. E. Green, W. J. Boettinger, H. E. Burdette and M. Kuriyama, "Asymmetric Crystal Topographic Camera," Rev. Sci. Instrum., Vol. 47, No. 8, August 1976.

4. T. S. Ananthanarayanan, R. G. Rosemeier, W. Mayo and J. H. Dinan, "Digital X-ray Rocking Curve Topography," MRS Fall Meeting, Boston, MA (December 1986).

5. T. S. Ananthanarayanan, "International Advances in Non-destructive Testing," Gordon & Preech, NY, Vol. 13, 1987.

6. R. E. Green, Adv. X-ray Anal., 20 (1977) 221.

7. T. S. Ananthanarayanan, W. E. Mayo and R. G. Rosemeier, "High Resolution Digital X-ray Rocking Curve Topography," submitted at the 35th Annual Denver Conference on Applications of X-ray Analysis, Denver, CO (1986).

8. A. Guinier, "X-ray Diffraction," W. H. Freeman & Co., 1963 ed., San Francisco.

9. B. W. Batterman and H. Cole, "Reviews of Modern Physics," Volume 36, No.3, July (1964).

Characterizing Process Induced Microstructural Damage in III-V Materials

T. S. Ananthanarayanan, J. I. Soos, R. G. Rosemeier, D. C. Leepa and A. L. Wiltrout

Brimrose Corporation of America, 7720 Belair Road, Baltimore, MD 21236

ABSTRACT: X-ray rocking curve analysis is emerging as a powerful technique for quantifying micro-lattice strain state. Ananthanarayanan, etal. (1986-1987) in the past have clearly demonstrated the efficacy of this technique for characterizing surface microstructural quality. The present study utilizes x-ray rocking curve topography to estimate process induced microstructural damage in materials such as GaAs and GaP. These materials are currently being used for sophisticated acousto-optic devices. Their surface/subsurface strain state is critical to device fabrication (transducer bonding) and performance. Several surface conditions obtained by varying the grinding/polishing grit size and Brinell hardness indentation have been evaluated by the digital automated rocking curve (DARC) topography technique. The 2-D topographic maps of Bragg peak shift, Bragg peak broadening and Bragg peak integrated intensity have been used to discern grown-in and process induced microstructural inhomogenieties. The DARC technique is amenable to advanced computing and artificial intelligence (AI) environments. Both research and production oriented application will significantly benefit from such a tool. Currently the entire analysis for a 1" wafer requires about 5 minutes at 100μm spatial resolution with a personal computer based system.

1. INTRODUCTION

Berg-Barrett (1945) x-ray diffraction topography is a fairly popular tool for evaluating single crystal microstructure. This technique is highly sensitive to microstructure and fairly rapid in execution. Several modifications to this technique have been developed to improve spatial and defect resolution such as ACT (Asymmetric Crystal Topography) by Green, etal. (1976) and Double Crystal topography by Bonze (1958). Typically with higher spatial resolution the diffracted beam intensity diminishes and so requires long data acquisition times. This study utilizes the state-of-the-art modification to the Berg-Barrett topography called rocking curve topography. This technique has been used to monitor process induced microstructural damage. Surface grinding/polishing and single point Brinell hardness indentation have been used to simulate process damage.

2. ROCKING CURVE TOPOGRAPHY

Rocking curve topography involves the combination of rocking curve analysis and diffraction topography. The diffracting domain of a given crystal is measured for a set of geometric conditions and x-ray beam optics. The diffracting domain of the crystal is a measure of the reciprocal volume of the crystal. The reciprocal volume is in-turn related to the micro-lattice structure of the crystal. In general (kinematic theory) the reciprocal

volume is inversely related to crystal perfection i.e., as the amount of defects (imperfections) increase the reciprocal volume (diffracting domain) increases. However, for special cases such as thin epitaxial films the above generalization will not be valid. It will be necessary to invoke the dynamic theory of x-ray diffraction in such cases. The measurement will still be appropriate but the analysis will be different. The current study uses the kinematic approach for the analysis. These substrates were prepared to minimize the effect of surface geometry on the rocking curve measurements. They were ground, polished and lapped with minimal surface curvature.

Ananthanarayanan and Trivedi have presented a detailed description of the hardware and software involved in digital rocking curve topography.

3. RESULTS & DISCUSSIONS

Figure 1 depicts the rocking curve topograph obtained from a GaP crystal with (111) surface orientation and two Brinell hardness indentations at 60kg preload. The series of Berg-Barrett topographs (over 0.5° rocking angle range at 0.1° interval) show the image contrast obtained with the conventional technique. Immediately below this series of topographs is the x-ray rocking curve half-width map obtained by analyzing the entire rocking range of the GaP crystal. The enhanced contrast due the the local disturbance in the crystal lattice state (microstructure) is evident. The 3-D perspective view of the rocking curve topograph also shows the crystal dimensions. The entire rocking curve analysis for this specimen took no longer than 40 secs.

Figure 2a depicts the rocking curve profiles obtained from a GaAs ((100) surface orientation) sample subjected to varying surface damage (by grinding) showing the K alpha 1 and K alpha 2 peaks for individual pixels. The cleaved surface was used as the starting surface for measuring grown-in defect density. This surface was then ground with several grinding grit sizes (40μm, 15μm, 9μm, 3μm, 0.3μm). The rocking curve measurements were made over the entire specimen at 100μm spatial resolution and the mean value over 10 X 10 pixels was computed to obtain the error bar at each data point in Figure 2b which shows the sensitivity of the rocking curve half width (unmonochromated) to surface grind.

In conclusion, the combination of the conventional 2-D Berg-Barrett topography with rocking curve analysis through digital data acquisition and image processing yields significantly enhanced defect contrast both grown-in as well as process induced. The non-destructive, non-contacting nature of this technique is the paramount advantage both in the production and research environments.

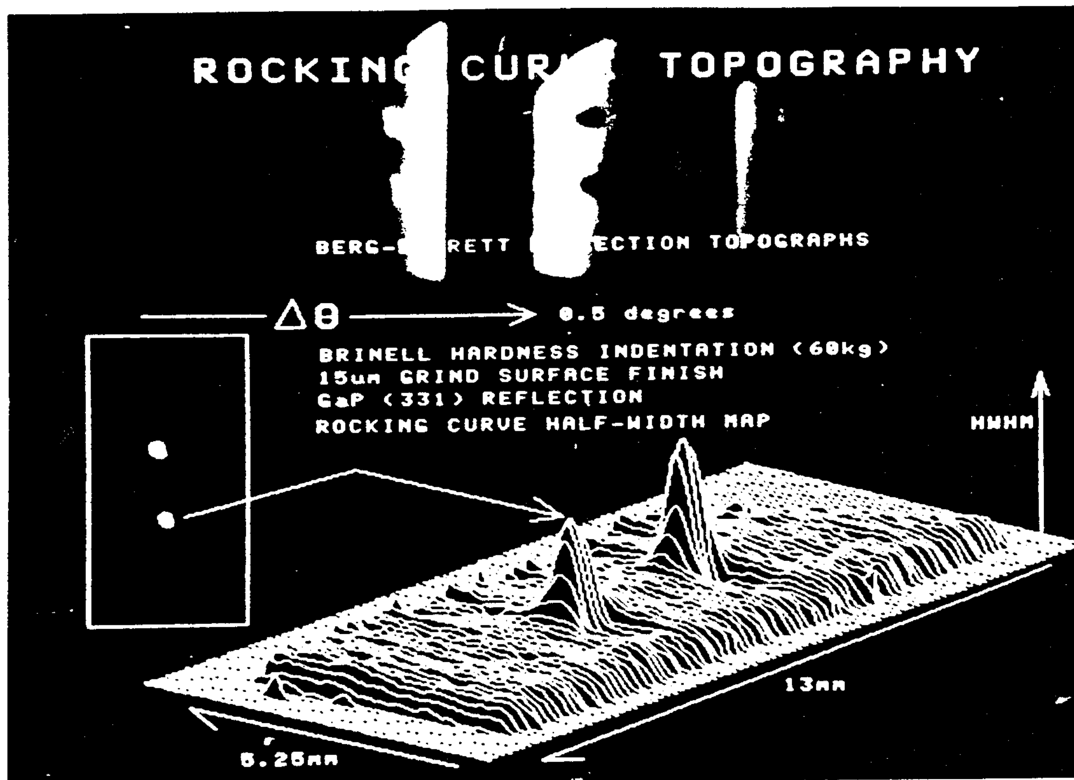

Figure 1: GaP (331) Berg-Barrett Topographs, Rocking Curve Half-width Map of Brinell Hardness Indentations Cu Radiation.

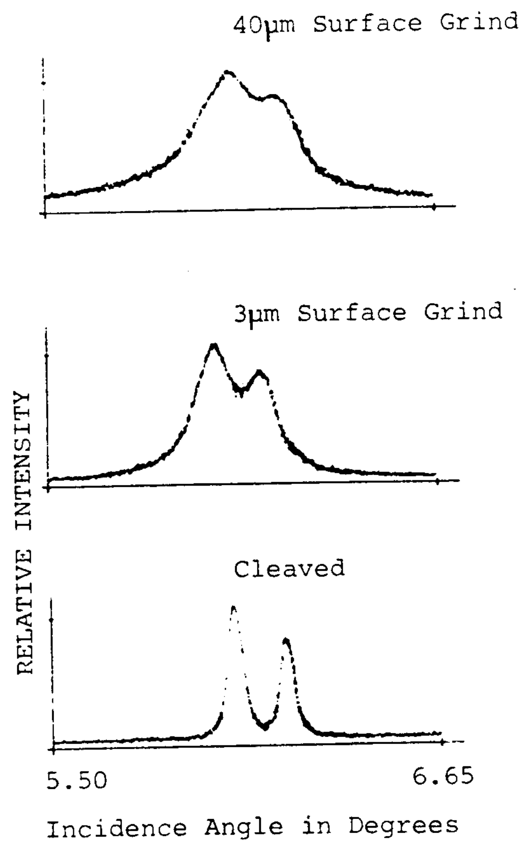

Figure 2a: Rocking Curve Pixel Profile GaAs (331) Cu Radiation.

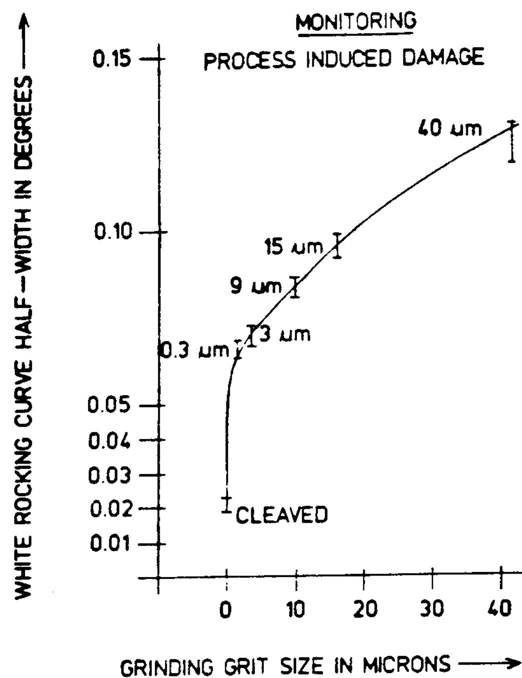

Figure 2b: GaAs (331) Rocking Curve, Cu Radiation.

4. REFERENCES

Ananthanarayanan, T. S., **Renaissance in X-Ray Diffraction Topography**, International Advances in Non-Destructive Testing, Gordon & Preech, NY, Vol. 13, 1987.

Ananthanarayanan, T. S, Rosemeier, R. G., Mayo, W. E. and Dinan, J. H., **Digital X-ray Rocking Curve Topography**, published in the 1986 MRS Proceedings, 1986.

Ananthanarayanan, T. S., Rosemeier, R. G., Mayo, W. E. and Becla, P., **Subsurface Micro-Lattice Strain Mapping**, published in the 1986 MRS Proceedings, 1986.

Ananthanarayanan, T. S. and Trivedi, S. B., **DARC, a Novel Topographic Technique for Rapid Non-destructive Characterization of III-V compounds**, Proceedings of DRIP II International Symposium on Defect Recognition and Image Processing in III-V Compounds, Monterey, Ca., 1987.

Barrett, C. S., **Trans. AIME**, Vol. 161, p15, 1945.

Green, R. E., Boettinger, W. J., Burdette, H. E. and Kuriyama, M., **Asymmetric Crystal Topography Camera**, Rev. Sci. Instr. Vol. 47, No. 8, 1976.

Bonze, U., **Z. Physik**, Vol. 153, p278, 1958.

RESEARCH SPONSOR: DEFENSE ADVANCED RESEARCH PROJECTS AGENCY (DARPA)

DIGITAL X-RAY ROCKING CURVE TOPOGRAPHY

T. S. Ananthanarayanan, R. G. Rosemeier, W. E. Mayo*, J. H. Dinan**

BRIMROSE, 7720 Belair Road, Baltimore, MD 21236.

* RUTGERS UNIV., Piscataway, NJ 08854.

** Army Night Vision Lab., Ft. Belvoir, MD 22160

SUMMARY

There is a considerable body of work available illustrating the significance of X-ray rocking curve measurements in micro-electronic applications. For the first time a high resolution (100-150μm) 2-dimensional technique called DARC (Digital Automated Rocking Curve) topography has been implemented. This method is an enhancement of the conventional double crystal diffractometer using a real time 2-dimensional X-ray detector.

Several materials have been successfully examined using DARC topography. Some of these include: Si, GaAs, AlGaAs, InGaAs, HgMnTe, Al, Inconel, steels, etc. By choosing the appropriate Bragg reflection multi-layered micro-electronic structures have been analyzed non-destructively. Several epitaxial films, including HgCdTe and ZnCdTe, grown by molecular beam epitaxy, have also been characterized using DARC topography. The rocking curve half width maps can be translated to dislocation density maps with relative ease. This technique also allows the deconvolution of the micro-plastic lattice strain component from the total strain tensor.

BACKGROUND

X-ray diffraction techniques for surface and near-surface microstructure characterization have shown enormous potential. These techniques have been developed over the past three or four decades. They have been principally qualitative in nature up until the recent past. The advent of digital X-ray detectors has clearly spurred these techniques into prominence.

Photographic films and emulsions were the most popular method of recording X-ray diffraction events. Lately, however, digital X-ray detectors are slowly but surely displacing film in numerous applications. The digital detectors include: point counters, linear array detectors and 2-dimensional detectors. The 2-dimensional detectors appear to be most versatile and effective for real time X-ray imaging. They have been successfully used for X-ray radiography and diffraction in several varied applications.

Some of the pioneering work in the application of 2-dimensional X-ray detectors has been conducted by Green et al.[1]. This work has been directed towards radiography, topography and transmission Laue diffraction. Green et al. have also used the 2-dimensional X-ray imaging system to qualitatively record the diffracting domain (rocking curve) of single crystals[2]. This group has conducted extensive experimentation in various metallurgical and crystallographic phenomena utilizing real time X-ray imaging[3]. Their work has lead to the wide acceptance of the 2-dimensional X-ray imaging device for recording X-ray diffraction events in a multitude of applications. Of specific interest currently is its application for X-ray rocking curve analysis and surface/subsurface micro-lattice strain mapping.

In recent years Weissman et al.[4] have used a unique technique for recording and mapping micro-lattice strain state using X-ray rocking curve analysis. This group originally utilized a cylindrical photographic film to record the intersections of the Ewald sphere and the reciprocal lattice. The analog film was replaced by linear array detectors to enhance digitization of the data. This system acronymed CARCA (Computer Aided Rocking Curve Analyzer) has already been discussed in great detail[5,6]. The limitation of the CARCA system is the enormous data acquisition time required.

EXPERIMENTAL PROCEDURE

The present study involves recording the reciprocal space volume using 2-dimensional X-ray image detectors[7-9]. The 2-dimensional imaging system used is based on multi-stage X-ray image intensifier and digital image processor technologies shown in Figure 1.

Figure 2 shows the schematics of the experimental setup used for the white beam X-ray rocking curve topography.

The incident beam impinges on the specimen at a shallow angle (1-8°). This allows the entire sample surface to be irradiated by the narrow incident beam. The diffraction geometry for the reflection topography is shown in Figure 3. The specimen is rocked about an axis contained on the specimen surface. The rocking is performed in precise step wise increments (minimum of 0.1 arc sec) and the reflection topograph digitally recorded at each step increment. The detector placed at the appropriate 2θ can record topographs of any desired (hkl) reflection from the crystal. Typical values of X-ray rocking curve half widths measured using white beam rocking curve topography range from 0.05 - 1°. At this point it should be recognized that by monochromating the incident beam, the rocking curve half width resolution can be improved at least two orders of magnitude. This has been established by many investigators in the past[10-12], however, white beam X-ray rocking curve topography used in this study gives reliable contour maps of the variation of X-ray rocking curve half width. The X-ray source used in this study was a very low power unit and hence required the direct incident beam (white beam) without beam attenuation which invariably accompanies the process of monochromation.

Once the entire reflecting domain has been recorded every individual pixel is analysed for rocking curve half width, Bragg peak shift and integrated intensity. This analysis is conducted on the image data stored in the computer. A powerful image processing system performs this pixel by pixel analysis through DMA (direct memory access). The results of the X-ray rocking curve half width and the Bragg peak shift are displayed topographically for each pixel. Thus a measure of the reciprocal lattice vector can be obtained for the entire specimen surface. The entire analysis can now be performed within 5 secs for a 20mm X 20mm area at 100-150μm spatial resolution.

PIXI Portable Image X-ray Intensifier

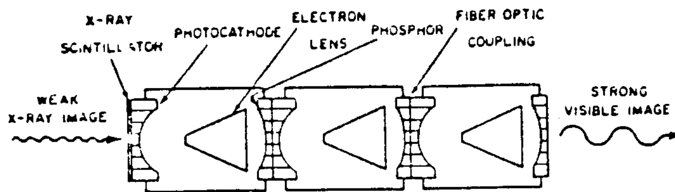

DIXIE Digital Intensity X-Ray Image Enhancer

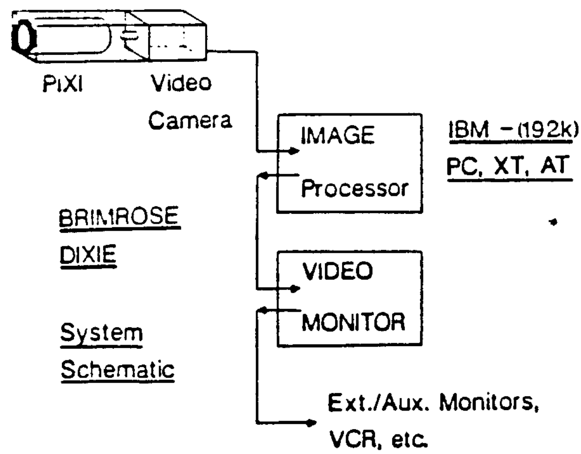

FIGURE 1 Digital 2-Dimensional X-ray Imaging System with a 3 Stage X-ray Image Intensifier.

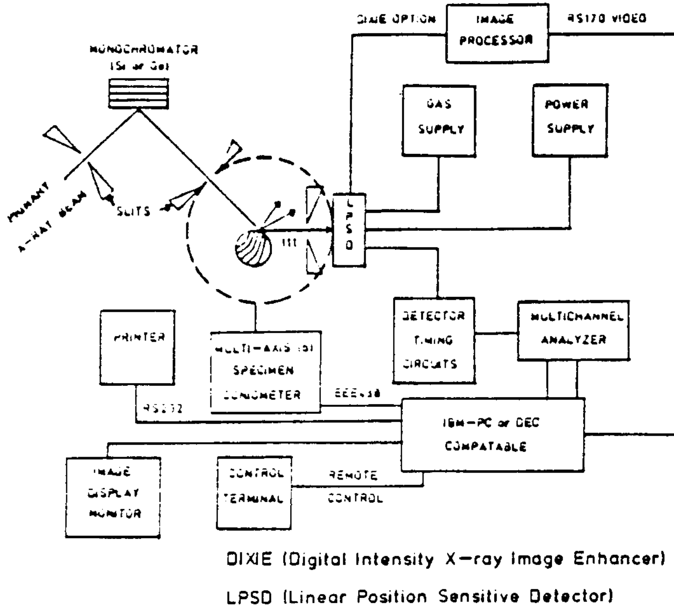

FIGURE 2 Schematic of Digital Rocking Curve Analyzer.

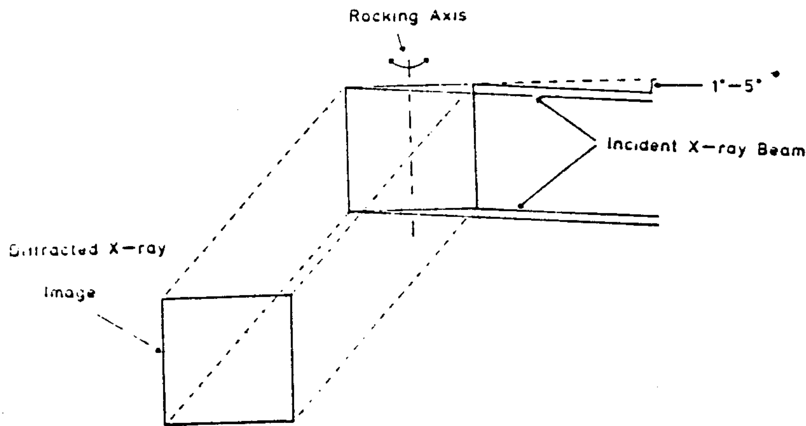

FIGURE 3 Diffraction Geometry for White Beam Rocking Curve Topography.

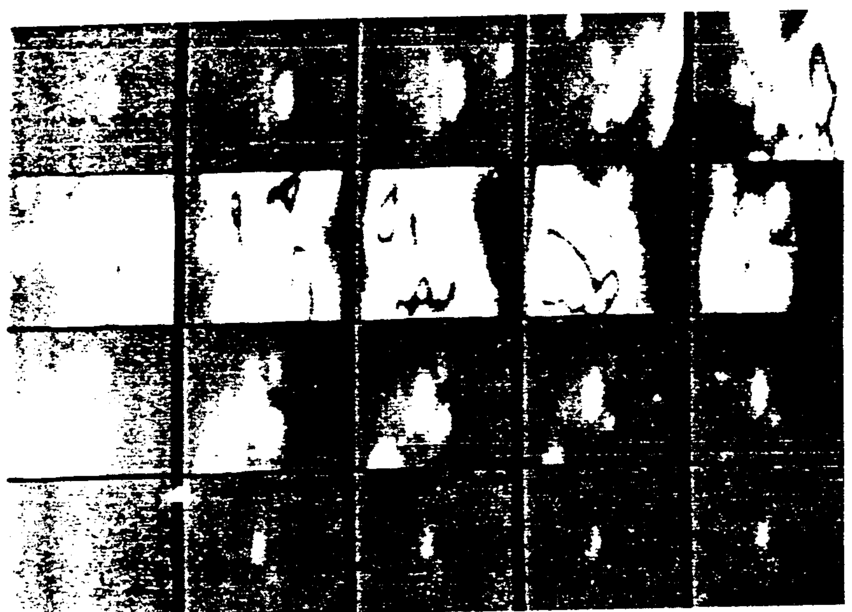

FIGURE 4a Cu K_α Radiation (510) Reflection $2\theta = 57.225°$
Surface Orientation (110), Incidence Angle 3° - 4°
$\Delta\theta$ (Angular Increment) between Frames = 0.10°.

10mm

BRAGG PEAK SHIFT MAP

BRAGG PEAK BROADENING MAP

FIGURE 4b Rocking Curve Topographs of the above NaCl Crystal. (Displays in Figure 4 and 5 are in color).

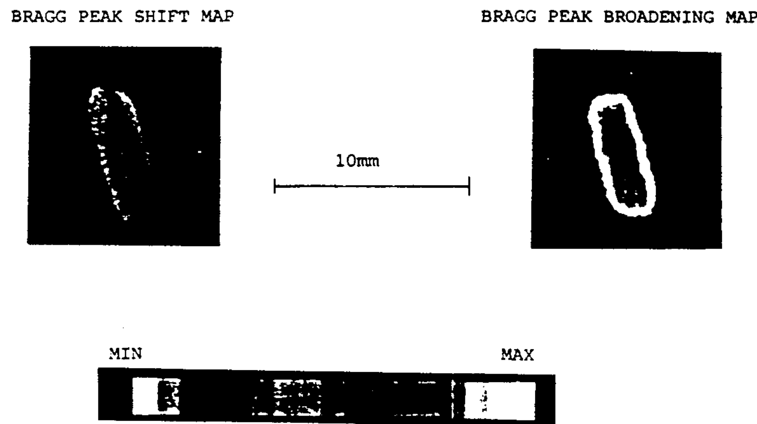

FIGURE 5 ZnCdTe EPI/InSb (111) Substrate Grown by MBE.
(010) Reflection, Cu K_α Radiation, 2-Theta = 57.5°
Incidence Angle 5°-7°
$\Delta\theta$ (Angular Increment) between Frames = .05°

RESULTS AND DISCUSSION

Figure 4a shows the (510) reflection rocking curve analysis from a NaCl crystal with a Brinel hardness indentation. This indentation was made with a 70kg preload. The Bragg peak broadening shown in Figure 4b clearly indicates the dislocation distribution around the indentation. The strain anisotropy along the (110) directions can also be seen. In contrast to the rocking curve half width map, the peak shift map has little correlation with the hardness indentation. This is reasonable because the effect of the indentation on the lattice parameter map (Bragg peak shift map) is minimal.

Figure 5 depicts the rocking curve topograph from a ZnCdTe epitaxy/InSb substrate grown by molecular beam epitaxy (MBE). This topograph shows dislocation striations formed either by the growth process and/or by twinning in the substrate. These striations have definite crystallographic orientation. Further analysis is required to accurately determine the origin of this pattern. $Cd_{.95}Zn_{.05}Te$ layers were grown by MBE on a {100} InSb substrate. Composition of the alloy layers was set by adjusting the temperatures of two effusion cells, one containing polycrystalline CdTe, other, elemental Zn. Additional details of substrate surface preparation and growth conditions are given elsewhere[13].

In conclusion DARC topography technique provides quantitative information about the micro-lattice strain inhomogenieties in various crystalline materials. These maps of the Bragg peak shift, Bragg peak broadening can be translated to appropriate micro-lattice strain maps. The integrated intensity under each pixel can also be used to determine epitaxial film thickness. The DARC technique is highly amenable to automation and on-line production applications.

REFERENCES

1. Green, R. E., Adv. X-ray Anal., 20 (1977) 221.

2. Green. R. E., W. J. Boettinger, H. E. Burdette and M. Kuriyama, "Asymmetric Crystal Topographic Camera," Rev. Sci. Instrum., Vol. 47, No. 8, August 1976.

3. Reifsnider, K. and R. E. Green, Jr., "An Image Intensifier System for Dynamic X-ray Diffraction Studies," Rev. Sci. Instr. 39, 1651, (1968).

4. Reis, A., J. J. Slade and S. Weissmann, J. Appl. Phys. Vol. 22, p. 655 (1951) J. J. Slade, Jr., and S. Weissmann, J. Appl. Phys. Vol. 23, p. 323 (1952).

5. Yazici, R., W. Mayo, T. Takemoto and S. Weissmann, J. Appl. Cryst., 16 (1983) 89.

6. Mayo, W., R. Yazici, T. Takemoto and S. Weissmann, XII Congress of Int. Union of Crystallography, 1981, Ottawa, Canada.

7. Ananthanarayanan, T. S., R. G. Rosemeier, W. E. Mayo and S. Sacks, "Novel Non-destructive X-ray Technique for Near Real Time Defect Mapping," submitted at the 2nd International Symposium on the Nondestructive Characterization of Materials, Montreal, Canada (1986).

8. Ananthanarayanan, T. S., W. E. Mayo and R. G. Rosemeier, "High Resolution Digital X-ray Rocking Curve Topography," submitted at the 35th Annual Denver Conference on Applications of X-ray Analysis, Denver, Colorado (1986).

9. Ananthanarayanan, T. S., W. E. Mayo, R. G. Rosemeier and S. Sacks, "Rapid Non-Destructive X-ray Characterization of Solid Fuels/Propellants," submitted at the 35th Annual Denver Coference on Applications of X-ray Analysis, Denver, Colorado (1986).

10. Dinan, J. H., S. B. Qadri, "Evaluation of Substrates of Growth of HgCdTe by Molecular Beam Epitaxy," J. Vac. Sci. Technol. A4 (4), Jul/Aug 1986.

11. Halliwell, M. A. G., M. H. Lyons, B. K. Tanner and P. Ilczyszyn, "Assessment of Epitaxial Layers by Automated Scanning Double Axis Diffractometry," Journal of Crystal Growt 65 (1983) p. 672-678.

12. Qadri, S. B. and J. H. Dinan, Appl. Phys. Lett. 47, 1066 (1985).

13. Dinan, J. H and S. B. Qadri, "Thin Solid Films," 131 (1985) 267.

SUBSURFACE MICRO-LATTICE STRAIN MAPPING

T.S. Ananthanarayanan, R.G. Rosemeier, W.E. Mayo* and P. Becla**

Brimrose Corporation of America
7720 Belair Road
Baltimore, MD 21236
(301) 668-5800

* Rutgers University
Piscataway, NJ 08854

** MIT, Francis Bitter National Magnet Lab
Cambridge, MA 02139

Synopsis

Defect morphology and distribution up to depths of 20um have been shown to be critical to device performance in micro-electronic applications. A unique and novel x-ray diffraction method called DARC (Digital Automated Rocking Curve) topography has been effectively utilized to map crystalline micro-lattice strains in various substrates and epitaxial films. The spatial resolution of this technique is in the the order of 100um and the analysis time for a $2cm^2$ area is about 10 secs. DARC topography incorporates state-of-the-art 1-dimensional and 2-dimensional X-ray detectors to modify a conventional Double Crystal Diffractometer to obtain color x-ray rocking curve topographs.

This technique, being non-destructive and non-intrusive in nature, is an invaluable tool in materials' quality control for IR detector fabrication. The DARC topographs clearly delineate areas of micro-plastic strain inhomogeniety. Materials analyzed using this technique include HgMnTe, HgCdTe, BaF_2 , PbSe, PbS both substrates and epitaxial films. By varying the incident x-ray beam wavelength the depth of penetration can be adjusted from a 1-2 micron up to 15-20um. This can easily be achieved in a synchrotron.

Background : II-VI Characterization and Use

II-VI compound semiconductors form a major family of compounds for advanced IR device applications. These include both active (laser generators) and passive (detector) devices. The compounds of interest may vary anywhere from a binary alloys to complicated multi-constituent epitaxies and heterostructures. The metallurgy involved in the crystallization of many of these multi-constituent, multi-layer materials is extremely complicated. Consequently, these materials tend to have higher defect structures than a single element material. Nevertheless, the consistency of any microscopic (electrical and mechanical) property is directly a function of the microlattice strain state. Hence there is increasing need for a quantitative, non-destructive microstructural characterization technique.

Over the past three decades X-ray diffraction and topography techniques have emerged as sturdy tools for rapid quality control of crystalline materials(1). X-ray reflection topography has regained prominence in the recent past(2). This technique lacked quantification. Several attempts were made to digitize the photographic records of the diffraction events. Although these efforts yielded excellent results, they were unsuitable for rapid surface characterization required under production environments. This limitation affects the data collection abilities for research environments as well.

The use of electronic X-ray detectors is becoming increasingly popular in the field of X-ray diffraction. These detectors include: point counters, linear array detectors and 2-dimensional array detectors. The principal detector used in this study is a 2-dimensional X-ray detector. Several studies(3-4) have clearly established the use of 2-dimensional X-ray detectors for real time topographic inspection of various metallographic microstructures(5-11). The current study utilizes 2-dimensional X-ray detectors to quantitatively map micro-lattice strain state in II-VI materials.

EXPERIMENTAL METHODOLOLGY

The technique used for surface characterization is known as X-ray rocking curve topography(6). The diffraction geometry used is shown in Figure 1.

The X-ray beam incident on the sample was not monochromated hence it contained $K\alpha_1$, $K\alpha_2$, $K\beta$ and some amount of Brehmstralung. The presence of other wavelengths cause multiple reflections ($K\alpha_1$, $K\alpha_2$, $K\beta$) and background noise. The signal to noise ratio and geometric divergence parameters diminish dramatically with increasing monochromation. Multiple crystal diffractometers can be used to achieve this(12).

The current study utilized no monochromators at all(13). Without monochromators the angular resolution of the micro-lattice misorientations achievable is limited. The specimen is then rocked (stepped) through its diffraction domain and every intersection of the Ewald sphere and the reciprocal lattice spot is recorded digitally. By tracking the X-ray intensity of each pixel, it is possible to record integrated pixel intensity, pixel rocking curve half width and pixel Bragg peak shift. Using these measurements the lattice parameters, dislocation density and epi-film thickness can be individually computed.

Figure 2 depicts the schematics of the rocking curve topography system and its configuration.

Figure 3 depicts the typical white beam rocking curve experiment performed on a VPE grown CdMnHgTe Epi/CdMnTe substrate. Angle of incidence was about 3-5o and the reflection topograph was obtained at about 54° two-theta. The reflection was found to be the 001 type. The angular increment between each frame was 0.1. Progressive frames begin left top corner and proceed right through the first row on to the second row (beginning left hand side again). The black and white images are translated to pseudo-color images and each pixel is tracked for intensity. Rocking curve half width for each pixel is obtained and displayed.

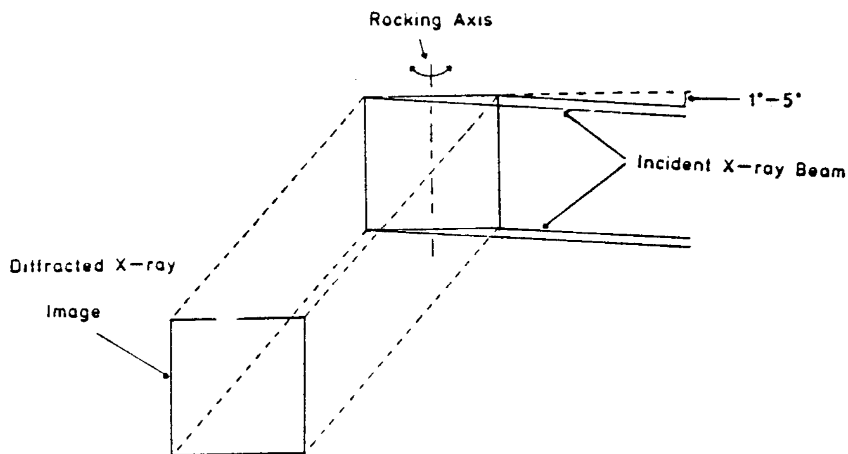

Fig. 1 DIFFRACTION GEOMETRY FOR WHITE BEAM ROCKING CURVE TOPOGRAPHY

DIGITAL AUTOMATED ROCKING CURVE TOFOGRAPHY

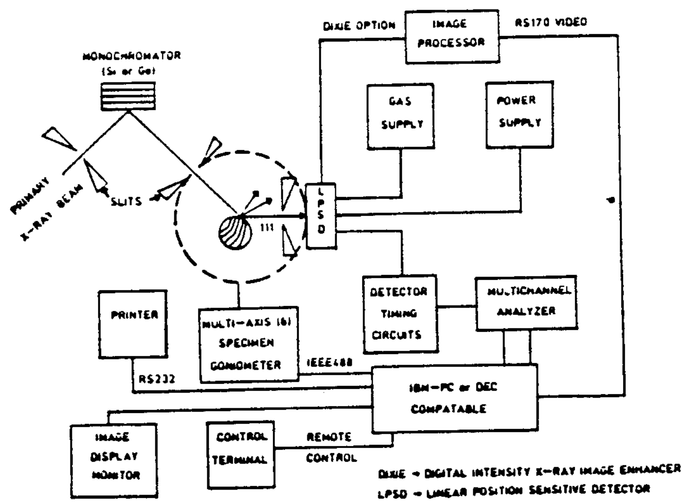

Fig. 2 Schematic of the Rocking Curve Topography System.

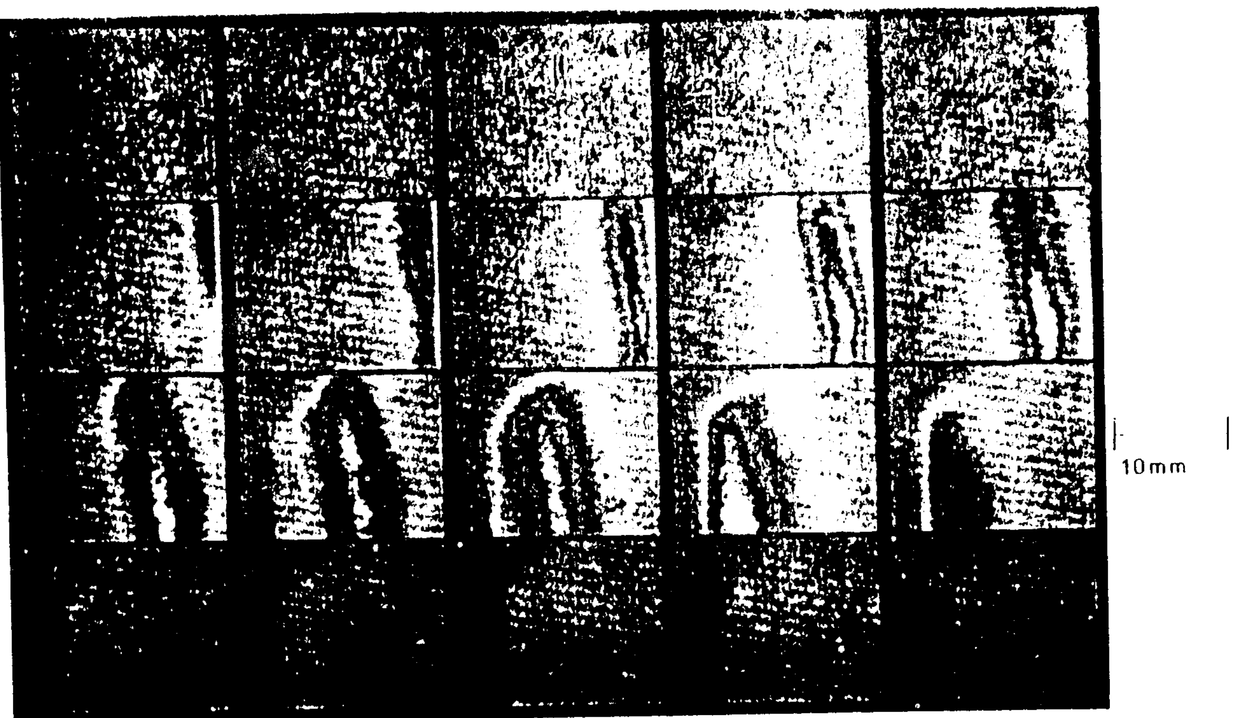

Fig. 3 Depicts Rocking Curve Experiment on a VPE Grown CdMnHgTe Epi/CdMnTe Substrate.

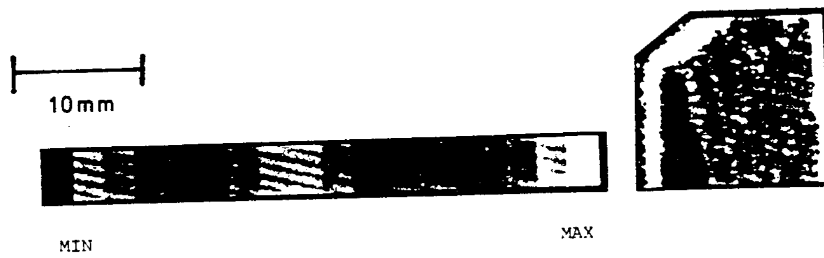

Fig. 4 Rocking Curve Topography of CdMnHgTe Epi/CdMnTe Substrate, (100) Type Reflection.

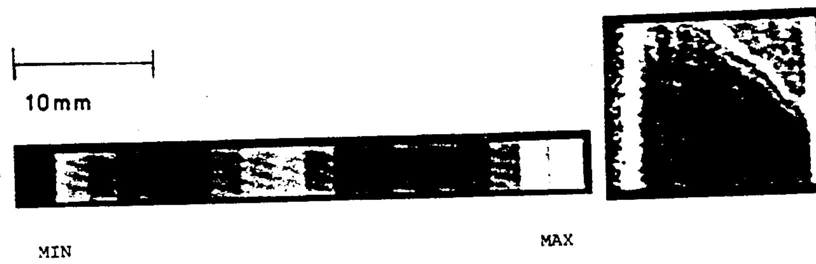

Fig. 5 Rocking Curve Topography of CdMnHgTe Epi/CdMnTe Substrate, (100) Type Reflection, on the Back Side.

Figure 4 is the rocking curve topography of the CdMnHgTe Epi/CdMnTe substrate. This topograph clearly shows subgrain structure in the VPE film. This film was about 250 um thick. The damaged area towards the edge of the speciment is also evident.

Figure 5 is the rocking curve topograph of the back side (CdMnTe substrate) of the sample in Figure 4. The substructure of the substrate is almost identical to the epi film. Also the fractured piece (which was removed for Figure 4) is clearly seen.

The epi substructure seems to identically duplicate that of its substrate. In conclusion the following features can be quantified using rocking curve topographs.

1. Deformation at specimen edges.
2. Cracks and microscopic discontinuities.
3. Subgrain structure.

ACKNOWLEDGEMENTS

The autho- wish to thank Alfred Wiltrout, Dawn Roche and Kathy Aversa for their assistance in compiling this manuscript. Special thanks to Dr. S. B. Trivedi for helpful discussions and Dr. P. J. Coyne for developing the software to implement digital rocking curve topography. This research effort was conducted under the sponsorship of DARPA, ONR and SPAWAR of the U.S. Dept. of Defense.

REFERENCES

1. Guinier, A., "X-ray Diffraction," W. H. Freeman & Co., 1963 ed., San Francisco.

2. Weissmann, S., "Recent Advances in X-ray Diffraction Topography," Fifty Years of Progress in Metallographic Techniques," Special Technical Publication No. 430.

3. Ananthanarayanan, T. S., W. E. Mayo and R. G. Rosemeier, "High Resolution Digital X-ray Rocking Curve Topography," to be published in Volume 30 of Advances of X-ray Analysis.

4. Ananthanarayanan, T. S., W. E. Mayo, R. G. Rosemeier and R. S. Miller, "Rapid Non-destructive X-ray Characterization of Solid Fuels/Propellants," to be published in Volume 30 of Advances of X-ray Analysis.

5. Pangborn, R., Ph.D. Thesis, Rutgers University, 1982.

6. Rosemeier, R. G., T. S. Ananthanarayanan and W. E. Mayo, "Feasibility Study on Real Time X-ray Topography - Phase I Final Report," DARPA, September 1984 - February 1985.

7. Mayo, W. E., R. Yazici, T. Takemoto and S. Weissmann, XII Congress of Int. Union of Crystallography, 1981, Ottawa, Canada.

8. Mayo, W. E., Ph.D. Thesis, Rutgers University, 1982.

9. Yazici, R., Ph.D. Thesis, Rutgers University, 1982.

10. Liu, H. Y., Ph.D. Thesis, Rutgers University, 1982.

11. Liu, H. Y., W. E. Mayo and S. Weissmann, Mat. Sci. and Eng., 63 (1984) 81.

12. Qadri, S. B., and J. H. Dinan, J. Appl. Phys. "X-ray Determination of Dislocation Density in Epitaxial ZnCdTe," p. 1066 (1985).

13. Ananthanarayanan, T. S., R. G. Rosemeier, W. E. Mayo and S. Sacks, "Novel Non-destructive X-ray Technique for Near Real Time Defect Mapping," submitted at the 2nd International Symposium on the Nondestructive Characterization of Materials, Montreal, Canada (1986).

From: ADVANCES IN X-RAY ANALYSIS, Vol. 30
Edited by Charles S. Barrett, John V. Gilfrich, Ron Jenkins,
Donald E. Leyden, John C. Russ and Paul K. Predecki
(Plenum Publishing Corporation, 1987)

HIGH RESOLUTION DIGITAL X-RAY ROCKING CURVE TOPOGRAPHY

T.S. Ananthanarayanan,[1] W.E. Mayo,[2] and R.G. Rosemeier[1]

[1]Brimrose Corp. of America, 7720 Belair Road, Baltimore, MD
[2]Rutgers University, Piscataway, NJ

ABSTRACT

This study presents a unique and novel enhancement of the double crystal diffractometer which allows topographic mapping of X-ray diffraction rocking curve half widths at about 100-150μm spatial resolution. This technique can be very effectively utilized to map micro-lattice strain fields in crystalline materials. The current focus will be on the application of a recently developed digital implementation for the rapid characterization of defect structure and distribution in various semiconductor materials.

Digital Automated Rocking Curve (DARC) topography has been successfully applied for characterizing defect structure in materials such as: GaAs, Si, AlGaAs, HgMnTe, HgCdTe, CdTe, Al, Inconnel, Steels, BaF_2, PbS, PbSe, etc. The non-intrusive (non-contact & non-destructive) nature of the DARC technique allows its use in studing several phenomena such as corrosion fatigue, recrystallization, grain growth, etc., *in situ*. DARC topography has been used for isolating regions of non-uniform dislocation density on various materials. It is envisioned that this highly sophisticated, yet simple to operate, system will improve semiconductor-device yield significantly.

The high strain sensitivity of the technique results from combination of the highly monochromated and collimated X-ray probe beam, the state of the art linear position-sensitive detector (LPSD) and the high-precision specimen goniometer.

INTRODUCTION

X-ray diffraction and radiography have been important tools for non-destructive materials' evaluation. A drawback in the entire field has been the lack of high-resolution direct X-ray imaging systems.

The authors have developed under past and present DOD sponsorship a highly advanced real-time digital 2-D X-ray imaging system. Some design details and descriptions of this system are also presented here.

Several X-ray diffraction techniques have been developed over the past four decades for examining surface and sub-surface crystal microstructure [1]. These techniques have been principally limited by the detector technology utilized in their implementation. Photographic film and the scintillation/proportional point counters have been the most popular X-ray detectors used thus far. These detectors require phenomenally long periods of time for data acquisition and have hence been tedious to use.

X-ray detection has been revolutionized with the advent of the unique new high resolution 1-D (linear) and 2-D (spatial) X-ray array detectors in combination with the powerful new micro-computer technology. The 1-D X-ray detector is based on the linear position sensitive detector technology. Recent research has extended the X-ray detectors to the 2-D arrays which are based on the CCD & X-ray image intensifier technology [2]. These 2-D detectors have similar spatial resolution as the 1-D detectors (100-150 microns). The power and analytical ability of several of these X-ray diffraction techniques have been amply demonstrated by numerous investigators. Some of these techniques include: X-ray diffractometry [1], X-ray topography [3], X-ray rocking - curve analysis [4] etc. These techniques can be effectively used to quantitatively measure the micro-lattice strain state in crystalline materials. The focus of the present study is X-ray rocking-curve analysis. This technique has been successfully utilized to map micro-plastic and micro-elastic strain in various substrates and epitaxial films namely; GaAs, AlGaAs, HgCdTe, CdTe, PbSe.

Some of the pioneering work in quantitative rocking-curve analysis was done by S. Weissmann et al. [4] at Rutgers University. This group initially utilized photographic film and photodensitometers to implement rocking-curve analysis. The film has recently been replaced by a linear position-sensitive detector [5]. The state-of-the-art 2-D X-ray digital detector has also been used by the authors in this study[6].

EXPERIMENTAL METHODOLOGY

The principal X-ray tool to be used in the investigation is a computerized double-crystal diffractomenter developed in great part with prior DOD funding[7-10]. This method, called the Computer Aided Rocking Curve Analyzer (CARCA), was pioneered at Rutgers University over the past few years[8-9] and has been shown to be of immense use in the determination of plastic strain distributions in both single-crystal and polycrystalline materials[8-11]. Since this method is unique and has only recently been disclosed in the literature, discussions of the method and its applications will be presented here.

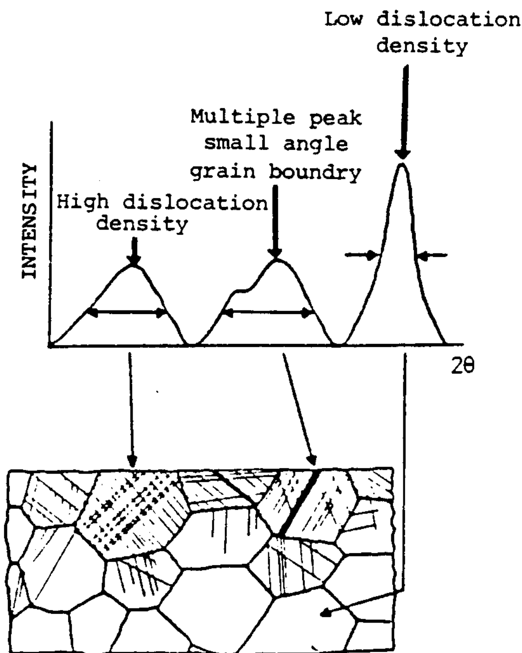

Figure 1. Schematic drawing showing the anticipated rocking curves for (a) grains with uniform distribution exhibiting a subgrain boundary, and (c) annealed grains with low excess dislocation density.

The method is based on the double crystal diffractometer in the (+n,-n) parallel arrangement. A monochromatic beam is produced by reflection from a (111) oriented Si crystal. After the $K_{\alpha 2}$-component is removed by the use of a long collimator and slit system, the highly monochromatic beam impinges on the test crystal. The test crystal is then rotated (or rocked) through its reflecting range and its intensity versus angular position is recorded. The rocking curve thus obtained is highly sensitive to the perfection of the lattice producing it as shown schematically in Figure 1. A relatively perfect region produces a sharp reflection with a narrow reflecting range indicated by a small B value (total width at half maximum intensity). If plastic deformation occurs, an excess number of dislocations of one sign are produced. If these are uniformly distributed, the rocking curve is broadened; but if the excess dislocations are non-uniformly distributed a multipeaked rocking curve is produced.

If the rocking curves can be determined on a point-to-point basis, for example by use of a microbeam combined with movement of the sample, a complete deformation map can be obtained. A more practical solution to the problem, however, is shown in Figure 2. Instead of using a microbeam, a large area of the specimen is irradiated by a parallel line source and advantage is taken of the

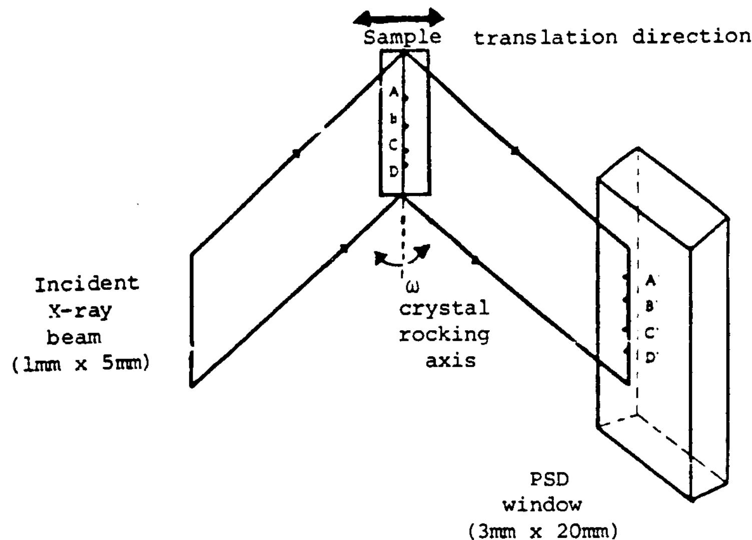

Figure 2. Showing orientation of PSD (Position Sensitive Detector) parallel to Debye-Scherrer arc.

fact that the diffracted beam line is a true topographic image. Accordingly, there is a one-to-one correspondence between the position in the diffracted-beam and the spot on the sample giving rise to it. This reflected beam is then registered by a linear position-sensitive detector (PSD) placed tangent to the Debrye arc and parallel to the rotation axis of the sample. When combined with a multichannel analyzer (MCA), the diffracted beam can be broken into 60 μm increments. Thus, as shown in Figure 2, the diffracted beam A′ originates from point A on the sample, and similarly for pairs BB′, CC′, etc. By step-rotations of the specimen, rocking curves are generated simultaneously and independently for each 60μm segment of the sample. When the rocking-curve analysis has been completed, the sample is step-wise translated so that adjacent regions can be similarly analyzed. In this way, a complete two-dimensional map can be readily generated in a few hours. A typical rocking-curve topograph of a InGaAs epitaxial film on a GaAs wafer is shown in Figure 3.

2-D X-RAY IMAGING

Professor Robert E. Green, Jr.[8] of the Johns Hopkins University in 1965 pioneered the first real-time electro-optical dynamic X-ray-image detection system which incorporated an external scintillator optically coupled to a magnetically-focused first-generation multi-stage image-intensifier tube. In 1968, Reifsnider and Green[1] developed a system incorporating an electrostatically-focused first-generation three-stage image-intensifier device (Figure 4a and 4b). Subsequently, this real time X-ray imaging device has shown many applications in the study of materials: grain-boundary migration

InGaAs Epitaxial Film

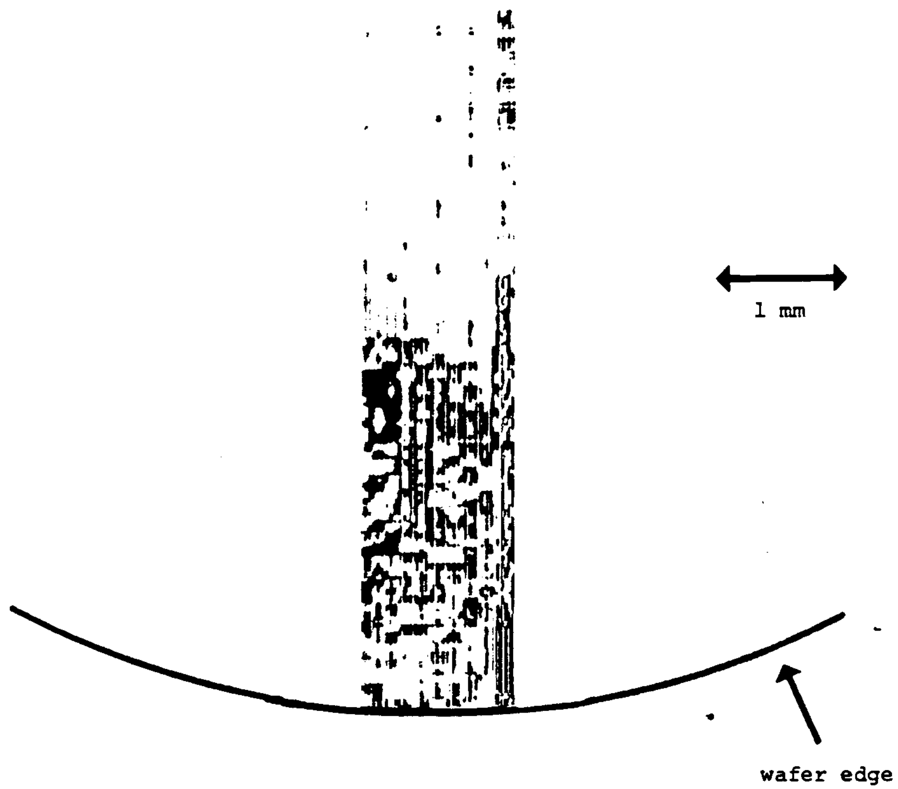

Figure 3. Plastic strain map or rocking curve topography obtained by the DARC technique; CuKα_1 radiation 400 reflection.

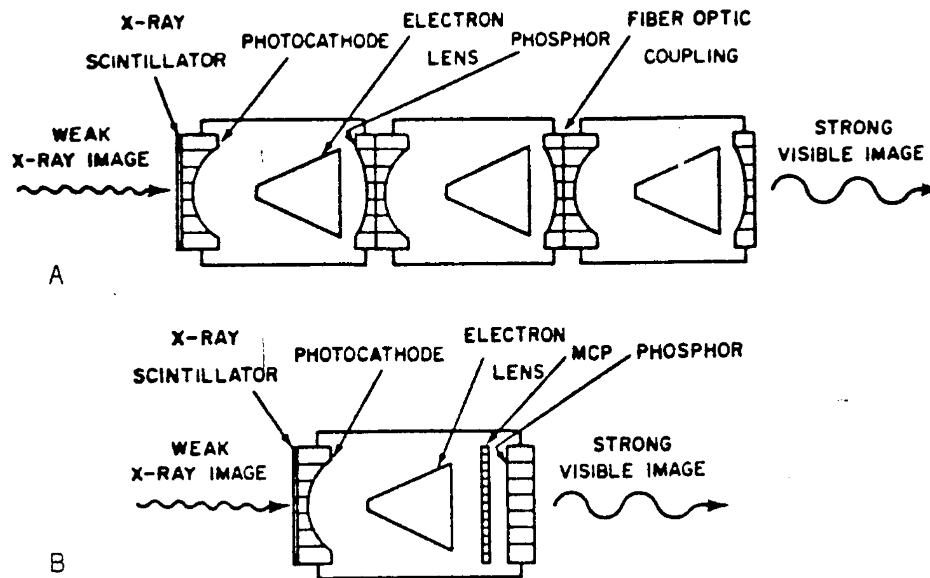

Figure 4. Schematic of (A) Portable Image X-ray Intensifier (PIXI) and (B) Miniature X-ray Intensifier (MINIX).

studies,[9] crystal-lattice rotation experiments,[10] solids undergoing shock-wave compression,[11] and topography.[2-5,12,13] However, applications in the medical and dental fields have been limited if not non-existent.

Other scientific investigators such as Reynolds, Milch, and Gruner[14] have developed a highly sensitive X-ray image-intensifier TV detector which incorporates a four-stage magnetically-focused

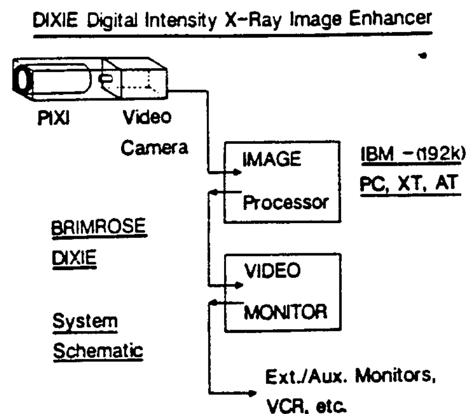

Figure 5. Schematic of the proposed digital real-time X-ray radiographic imaging system.

image intensifier coupled with a silicon target vidicon. This system has been used for biological X-ray experiments. Also, Bilderback[15] has developed a two-dimensional, area multiwire proportional detector that enables X-ray Laue back-reflection patterns to be observed in seconds. To the author's knowledge this system is commercially available. In 1978 Yin and Seltzer[16] developed a self-contained radiation source and imaging detector for real-time radiography. This system incorporates a microchannel-plate detector with a 25mm input X-ray window. The authors have further developed the X-ray image intensifier into a digital-intensity X-ray image-enhancer (DIXIE) using a digital video-camera and an image-processor. The image-processor allows the use of pseudo-color to depict intensity contours for easier visual inspection of images with multiple gray levels. The digital X-ray diffraction images obtained thus can be used to quantify microstructural defects. Figure 5 shows the schematic representation of the X-ray imaging system. It is possible to evaluate lattice-strain states in various crystalline materials in the topographic mode. X-ray topographs (pseudo-color intensity-contour maps) obtained with a camera system constructed for a conventional laboratory X-ray source[18] (3kW) are depicted in Figure 6.

In addition to X-ray diffraction imaging, the system can be very effectively utilized for high-resolution micro-radiography. Due to the enormous intensity of a synchrotron X-ray source, transmission Lang topography and anomalous X-ray scattering phenomena can also be studied. These techniques have great potential for characterizing thin-film (epitaxial) structures such as used in IR detectors. The DIXIE has now replaced the linear PSD in the DARC topography system. This enhancement will allow near-real time rocking-curve topography (5 secs for 1 inch square area).

CONCLUSION

Rocking-curve analysis is a powerful microstructural QC tool when implemented in a topographic mode. This technique can be effectively used to quantitatively map dislocation-density and lattice-parameter changes in both substrate and epitaxial films. By changing the X-ray wavelength it is also feasible to non-destructively evaluate substrate micro-lattice strain states below thin epi-taxial films. Using 2-D X-ray detectors the data acquistion time can be phenomenally improved (by 5 orders of magnitude). The technique is ideally suited for on-line production as well as sophisticated research applications.

ACKNOWLEDGEMENT

This research was sponsored by DARPA under contract #4941/6-20-84. The authors wish to express their gratitude to R. A. Reynolds and S. Roosild for their support in this project.

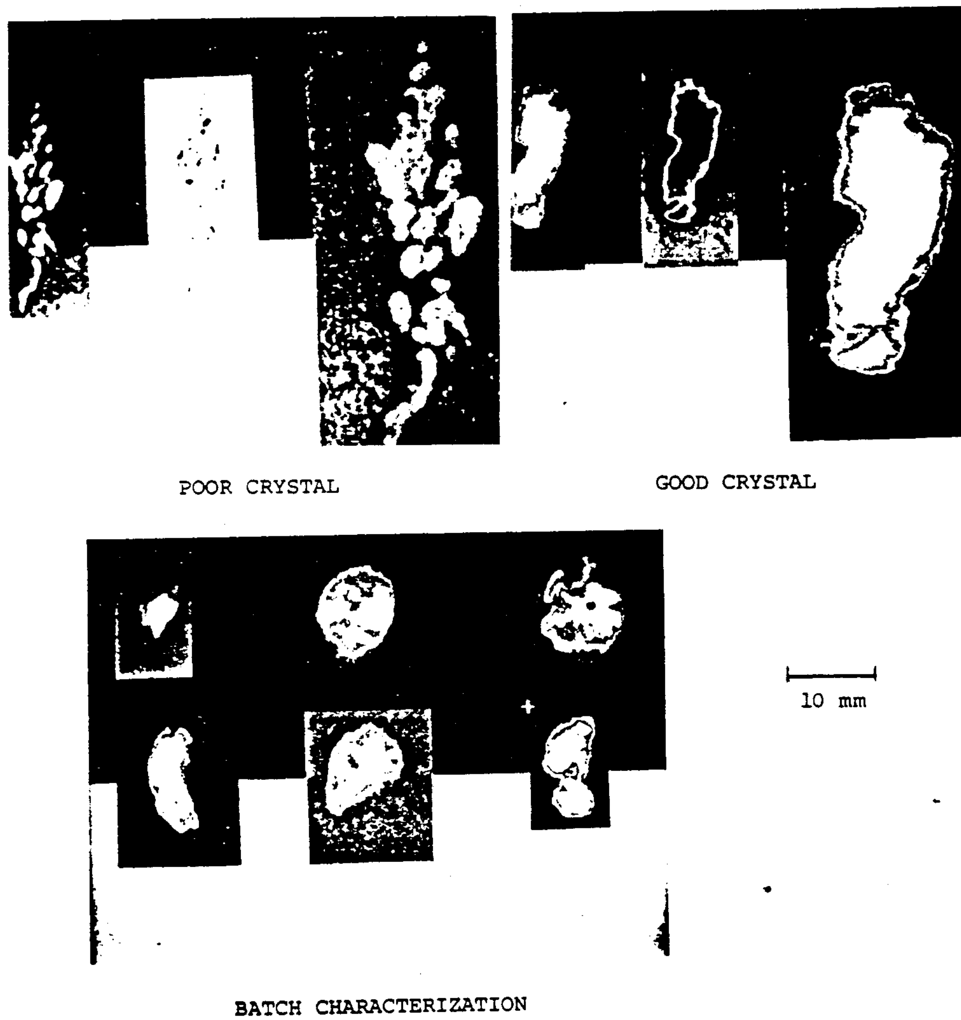

Figure 6. DIXIE - Digital Intensity X-ray Image Enhancer. Real-time topographs (HgMnTe).

REFERENCES

1. Guinier, A., "X-ray Diffraction", W. H. Freeman & Co., 1963 ed., San Francisco.

2. Reifsnider, K., and R. E. Green, Jr., "An Image Intensifier System for Dynamic X-ray Diffraction Studies," Rev. Sci. Instr. 39, 1651, (1968).

3. Weissmann, S., "Recent Advances in X-ray Diffraction Topography," Fifty Years of Progress in Metallographic Techniques," Special Technical Publication No. 430.

4. Reis, A., J. J. Slade and S. Weissmann, J. Appl. Phys. Vol. 22, p. 655 (1951) J. J. Slade, Jr., and S. Weissmann, J. Appl. Phys. Vol. 23, p. 323 (1952)

5. Pangborn, R., Ph. D. Thesis, Rutgers University, 1982

6. Rosemeier, R. G., T. S. Ananthanarayanan and W. Mayo, "Feasibility Study on Real Time X-ray Topography - Phase I Final Report", DARPA, September 1984 - February 1985.

7. Mayo, W., Yazici, R., Takemoto, T. and Weissmann, S., XII Congress of Int. Union of Crystallography, 1981, Ottawa, Canada.

8. Mayo, W., PH. D. Thesis, Rutgers University, 1982.

9. Yazici, R., Ph. D. Thesis, Rutgers University, 1982.

10. Liu, H. Y., Ph. D. Thesis, Rutgers University, 1982.

11. Liu, H. Y., W. E. Mayo and S. Weissmann, Mat. Sci. and Eng., 63 (1984) 81.

From: ADVANCES IN X-RAY ANALYSIS, Vol. 31
Edited by Charles S. Barrett, John V. Gilfrich, Ron Jenkins,
John C. Russ, James W. Richardson, Jr. and Paul K. Predecki
(Plenum Publishing Corporation, 1988)

PC BASED TOPOGRAPHY TECHNIQUE

Douglas C. Leepa
Brimrose Corp.
Baltimore, MD.

T. S. Ananthanarayanan
Brimrose Corp.
Baltimore, MD

Paul J. Coyne
Loyola College
Baltimore, MD

INTRODUCTION

This paper discusses the use of a personal computer in the x-ray diffraction laboratory. DARC (Digital Automated Rocking Curve) Topography is a system in which a PC is used extensively. Using this system as an example, the many uses and benefits of the PC as a tool will be explained.

Overview of the DARC Topography

Digital Automated Rocking Curve Topography is the digital recording of the Bragg reflection for every incidence angle position of a crystalline wafer that is rotated through a fixed pivot. The rocking axis is parallel to the crystallographic plane being interrogated. The incidence angle is usually in the range of 0.1 to 5 degrees. Unmonochromated copper radiation is used as the x-ray source, and an x-ray image intensifier is positioned to detect a particular diffraction topograph.[1] Other experiments have shown that this system is highly sensitive to microstructure.[2] One study has shown that a sample satisfies the Bragg condition over a much larger change in incidence angle after it has been deformed with a hardness indentation in comparison to the undeformed state. Since no other parameters were varied, this clearly points to a change due to a higher dislocation density. Further interpretation of the results and calculations made by the system require extensive study and will not be discussed here.[2]

SYSTEM HARDWARE

The DARC system utilizes an IBM PC/XT/AT or compatible computer with at least 512 kilobytes of RAM, an 8087 or 80287 coprocessor, a GPIB controller board, and an image acquisition and processing board with both grey composite and pseudocolor outputs. A hard disk drive is used for increased image storage area and improved data retrieval time. Two video monitors are used; one for displaying images, both real and processed, and the other for interfacing with the user as the data display terminal. A CCD (charge coupled device) camera with a standard RS-170 output is used as the input device to the image acquisition board. This camera is mounted to a

x-ray image intensifier. The output screen of the intensifier provides input for the CCD. Spatial resolution with this system is in the 100 to 150 micron range. Currently, a new detector is being evaluated for use with the system. This device is a thermo-electrically cooled x-ray sensitive CCD. Spatial resolution with this new camera is expected to be in the 20 to 30 micron range, thus allowing improved defect recognition. Four motorized translation stages are used to manipulate the sample within the beam of x-rays. The driving motors are actuated and monitored by a computer programmable motor controller which is linked to the personal computer via IEEE-488 interface.

USE OF THE PC

The PC is used to control the position of the sample via motors, acquire and analyze image data, display calculated results and store any selected data on hard or floppy disk. All of these functions are initialized or bypassed using control codes sent from the computer keyboard.

Motor Control

A principal function of the computer is to control and monitor the motion of the four axis translation stages. Both commands and data are transferred back and forth from the PC to a programmable motor controller via an IEEE-488 standard data bus. The PC is transformed into a GPIB controller by means of a commercially available expansion card. This addition can be easily configured and installed into most PC's. When the system is initialized, the computer instructs the motors to displace the stages to their home or starting positions, thus ensuring a consistent reference point and allowing both a higher degree of accuracy and precision. Once the stages have been set in place the experiment begins. During the data acquisition period, the motor that controls the incidence angle of the crystal is stepped a certain number of degrees a specified number of times. For example, if the experiment requires 101 images of the sample through 0.5 degrees, then after each image acquisition, the stage must be rotated 0.005 degrees or through 18 seconds of arc. The incidence angle is always increased during the acquisition period. Once the experiment is complete, the motor returns the stage to its starting incidence angle. It remains at rest until another experiment is started.

Image Acquisition, Evaluation, and Display

The image acquisition and processing board is also an internal computer expansion card. This board is responsible for digitizing the video images sent to it via RS-170 by the CCD camera. It is also the board which converts all image output data into analog composite and pseudocolor images for display on the system image monitor. The board is able to grab anywhere from one pixel to an entire screen of 512 x 480 pixels. Choosing only a selected area of the image eliminates the acquisition of unwanted and unnecessary data, increases the overall system speed, and reduces memory requirements. Preset and user-modified look-up tables provide a vast array of output possibilities and therefore more data from which the examined crystal's properties can be evaluated.

The analysis begins after the data has been acquired. The control program calculates three parameters from the experiment: peak broadening, peak shift, and integrated intensity. No interpretation of these calculations is made by the program, only the results are displayed. The

peak broadening map is calculated from each pixel's change in intensity as the incidence angle is increased. The DC background noise level is subtracted from each point on the profile, then the half height-half width of the peak profile is calculated. This is done for each pixel. The Peak Shift map is a display of the angle at which each pixel is at its maximum intensity value. A pixel with a peak intensity at a larger incidence angle will be displayed as a higher grey-scale level. Accordingly, a pixel that peaks at a smaller incidence angle will be displayed as a lower grey-scale level on this map. The integrated intensity is simply a display of the average intensity of each pixel over the rocking curve. In the program display, all result maps are enhanced to utilize the full available grey scale, but the results maps are saved as unenhanced data.

Full wafer mapping is accomplished by performing the analysis on different parts of the same sample rotated through the same angles, and saving the maps. Each time a section is analyzed the system returns itself to that area. From there, the collection window can be moved to a different part of the sample. Saved data can later be recalled piece by piece. Each section is displayed on the screen at the same location from which the data is taken. These larger maps can then be enhanced or expanded over the available dynamic range (grey levels) of the image processor and redisplayed in order to enhance hidden details.

The system's dual monitor configuration allows simultaneous viewing of the images and control of the experiment. All identification and experimental parameters are controlled, modified, and displayed at the terminal; the data are viewed on the image monitor.

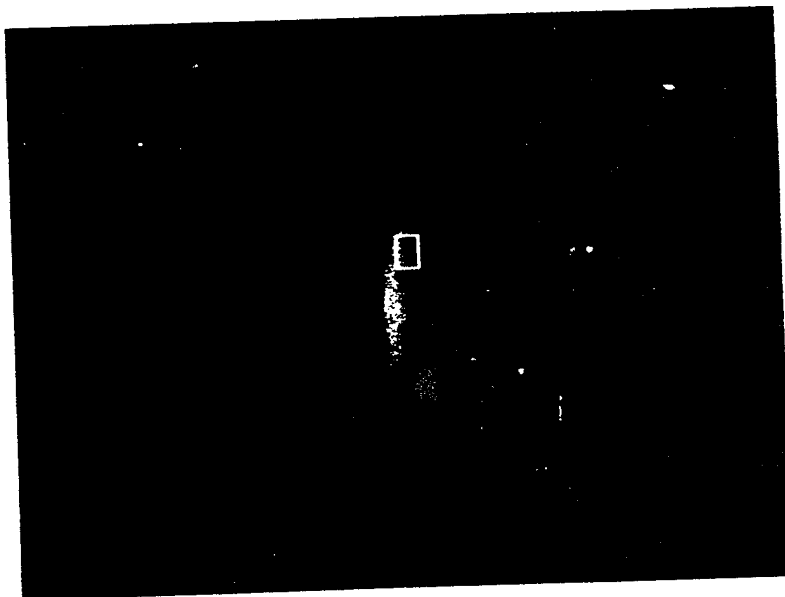

FIGURE 1

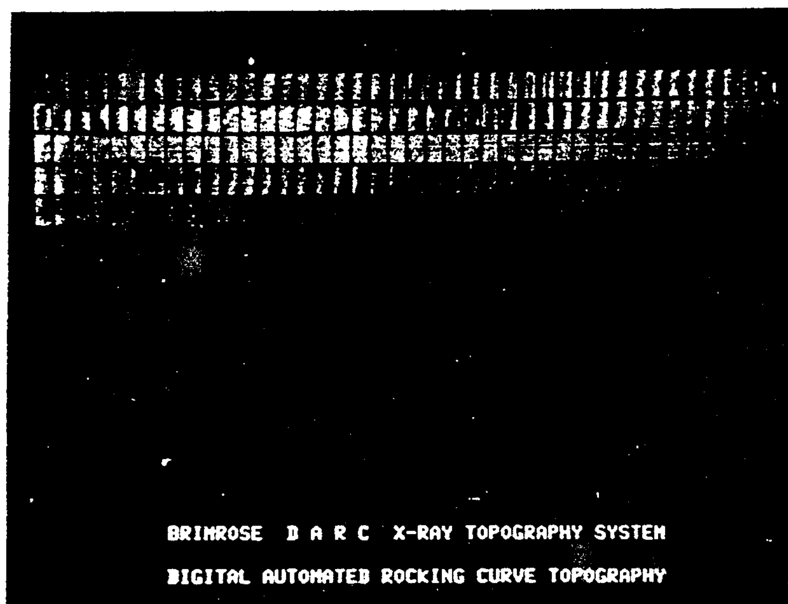

FIGURE 2

ANALYZED SAMPLES

The reflection topograph of a sample of Gallium Arsenide is shown in Figure 1. A data collection window is selected and the experiment is initiated. When the run is completed, the collected images are displayed, as illustrated in Figure 2. Each figure is a topograph of the sample taken from a different angle. The first window, in the upper left, coincides with the initial incidence angle; the last window, in the bottom right, with the

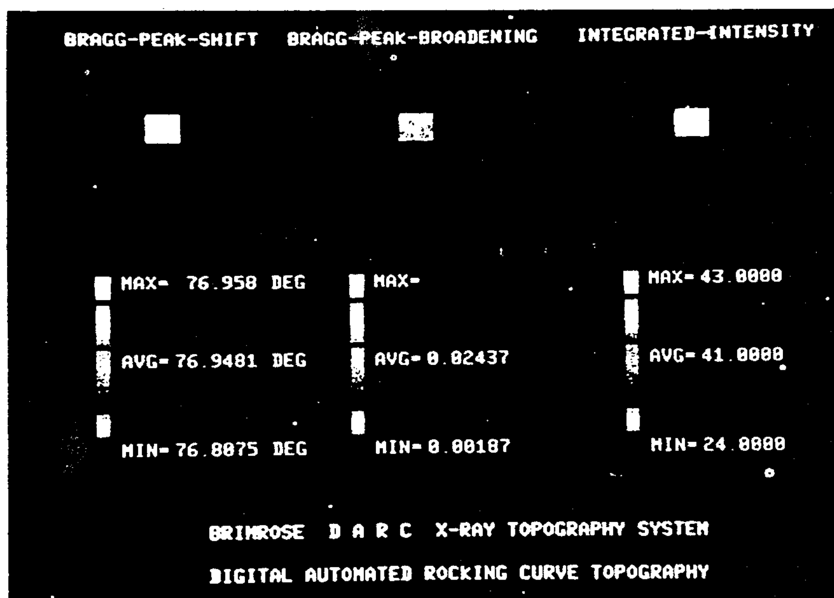

FIGURE 3

FIGURE 4

final incidence angle. At this point, the decision is made to use the data or to start over again. When sufficient data is obtained, the peak shift, peak broadening, and integrated intensity maps are displayed along with color bars providing visual reference points and numerical values with which the data may be analyzed, which is presented in Figure 3. Smaller step

FIGURE 5

sizes may also be used to increase angular resolution. The pixel profiles of the images obtained can also be viewed. These profiles are the raw data collected by the system. Profiles can be displayed singly, overlayed one by one, such as in Figure 4, or displayed for an entire row/column of pixels, as shown in Figure 5. The latter two allow comparison of data points.

Full wafer maps of Gallium Arsenide with devices are shown in Figures 6 and 7. Figures 6a, 6b and 6c show the peak shift, peak broadening (which is almost unobservable in this picture except for a small portion of the right most edge) and integrated intensity maps as raw data, and Figures 7a, 7b and 7c depict all three sets of data after being expanded over the available dynamic range. Pseudocolor is also used in order to bring out

PEAK SHIFT MAP

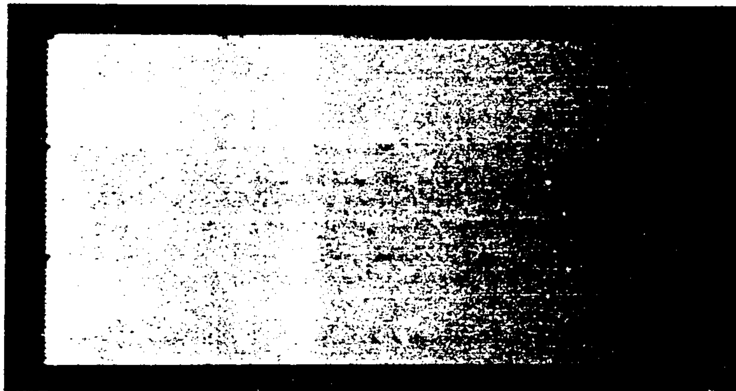

GaAs with Devices
FIGURE 6A

PEAK BROADENING MAP

GaAs with Devices
FIGURE 6B

INTEGRATED INTENSITY MAP

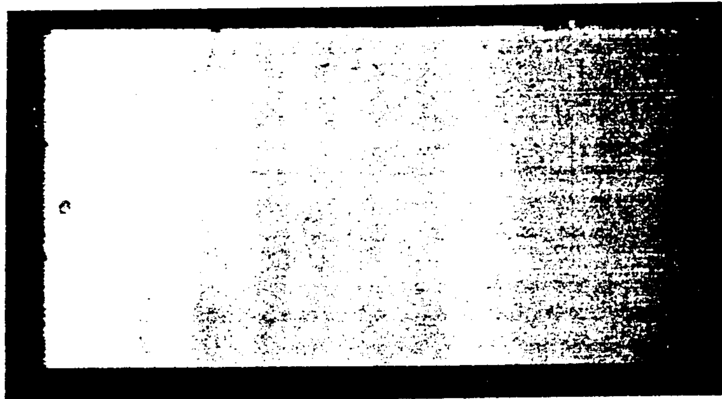

GaAs with Devices
FIGURE 6C

PEAK SHIFT MAP

(Expanded over Dynamic Range)

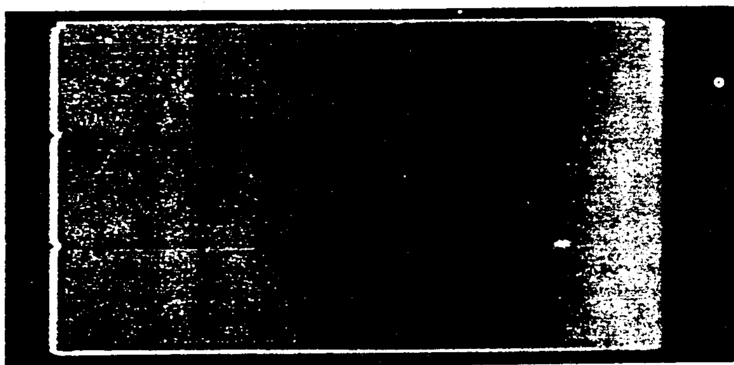

GaAs with Devices
FIGURE 7A

PEAK BROADENING MAP

(Expanded over Dynamic Range)

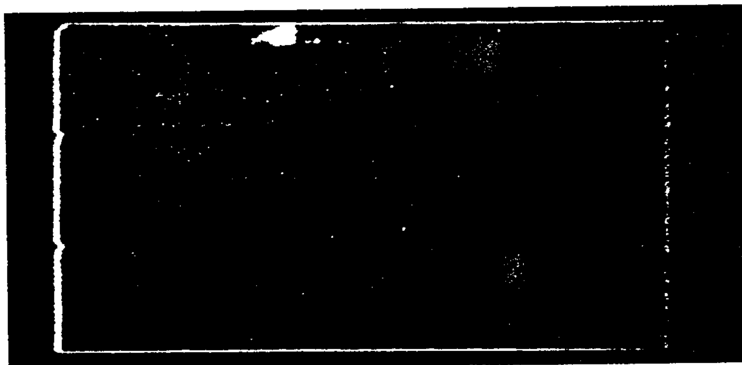

GaAs with Devices
FIGURE 7B

INTEGRATED INTENSITY MAP

(Expanded over Dynamic Range)

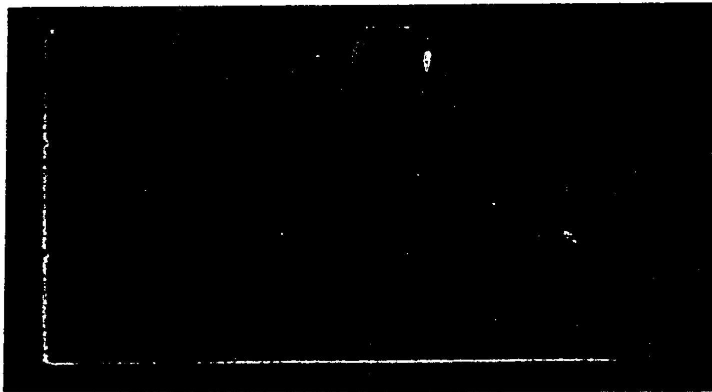

GaAs with Devices
FIGURE 7C

details that cannot be seen in standard black and white. Because of the increased contrast levels, slight variations in intensity become more noticeable to the eye. It is obvious that enhanced full wafer maps provide a superior analysis tool to the materials scientist by allowing high angular and spatial resolution data to be obtained separately and pieced together to present a detailed map of the crystal structure.

CONCLUSIONS

PC's have become indispensable to the x-ray community. Their ability to make numeric calculations and control experimental variables with great precision and speed has drastically reduced the time required to collect data on crystalline materials. The time required to obtain a two-dimensional rocking curve map of a 4 mm x 4 mm sample, with up to 1280 angular increments per run, has been cut from 1500 hours (with conventional point counters or linear point sensitive detectors) to five minutes with the DARC system. PC controlled experiments in real time Laue transmission and powder diffraction have proven very useful in material quality control.[3] With the low cost and high availability of expansion boards, the PC has become the workhorse of today's x-ray diffraction lab.

REFERENCES

1. T. S. Ananthanarayanan and S. B. Trivedi, "DARC, A Novel Topographic Technique for Rapid Non-Destructive Characterization of III-V Compounds," Elsevier Publishing Co., Monterey, CA (1987).
2. T. S. Ananthanarayanan, "Renaissance in X-Ray Diffraction Topography," Gordon & Preech, NY (1987).
3. T. S. Ananthanarayanan, S. B. Trivedi, R. G. Rosemeier, "Characterization of Solid Propellant Composites," The Non-Destructive Information Analysis Center, San Antonio, TX (April, 1987).

brimrose

APPENDIX B

COLOR PRINTS

WAFER 1: 3 micron of AlGaAs on GaAs grown by MBE. Conventional measurements predict no strain between substrate and epi layer.

PRINT 1A: Topograph where theta = 30 degrees and the incidence angle = 0.9 degrees. The black box indicates the area of interrogation.

1B: Pixel profile across center of box. Different color curves represent different horizontal points. As the substrates peak location moves, so follows the epi layers peak. Though this may mean a non-uniform substrate, this does indicate a good match between the two: no strain.

WAFER 2: Outer edge piece of a sliced wafer of single crystal InP.

PRINT 2A: Topograph where theta = 30 degrees and the incidence angle = 1.5 degrees.

2B: Incidence Angle and Peak Broadening maps concur that the best reflection is away from the outer edges and towards the center of what would be a full wafer (the lower right corner).

WAFER 3: GaAs wafer with twin defect.

PRINT 3A: Topograph where theta = 32 degrees and the incidence angle = 1.13 degrees.

3B: Topograph where theta = 32 degrees and the incidence angle = 1.19 degrees.

3C: Peak Shift and Peak Broadening maps show growth striations.

3D: Plot profile of fair crystals, but definite twins.

PRINT 1A

MBE-249

BRAGG-PEAK-SHIFT   BRAGG-PEAK-BROADENING   INTEGRATED-INTENSITY

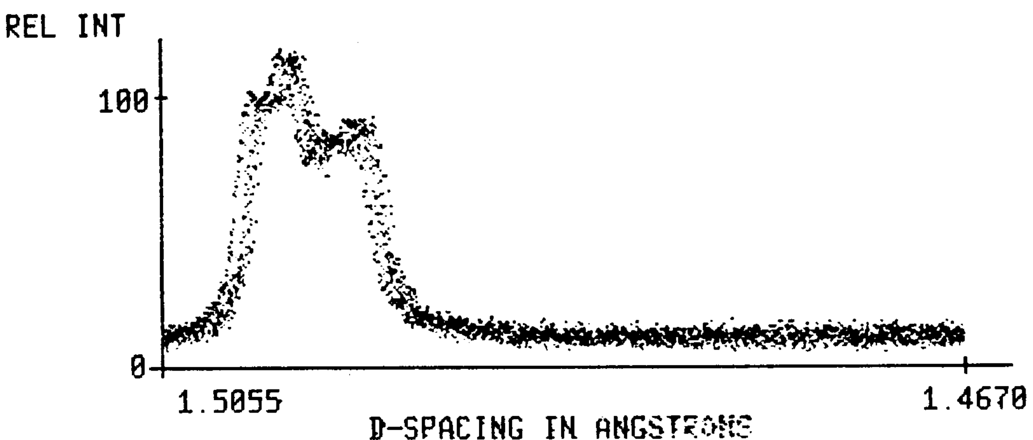

BRIMROSE D A R C X-RAY TOPOGRAPHY SYSTEM

DIGITAL AUTOMATED ROCKING CURVE TOPOGRAPHY

PRINT 1B

PRINT 2A

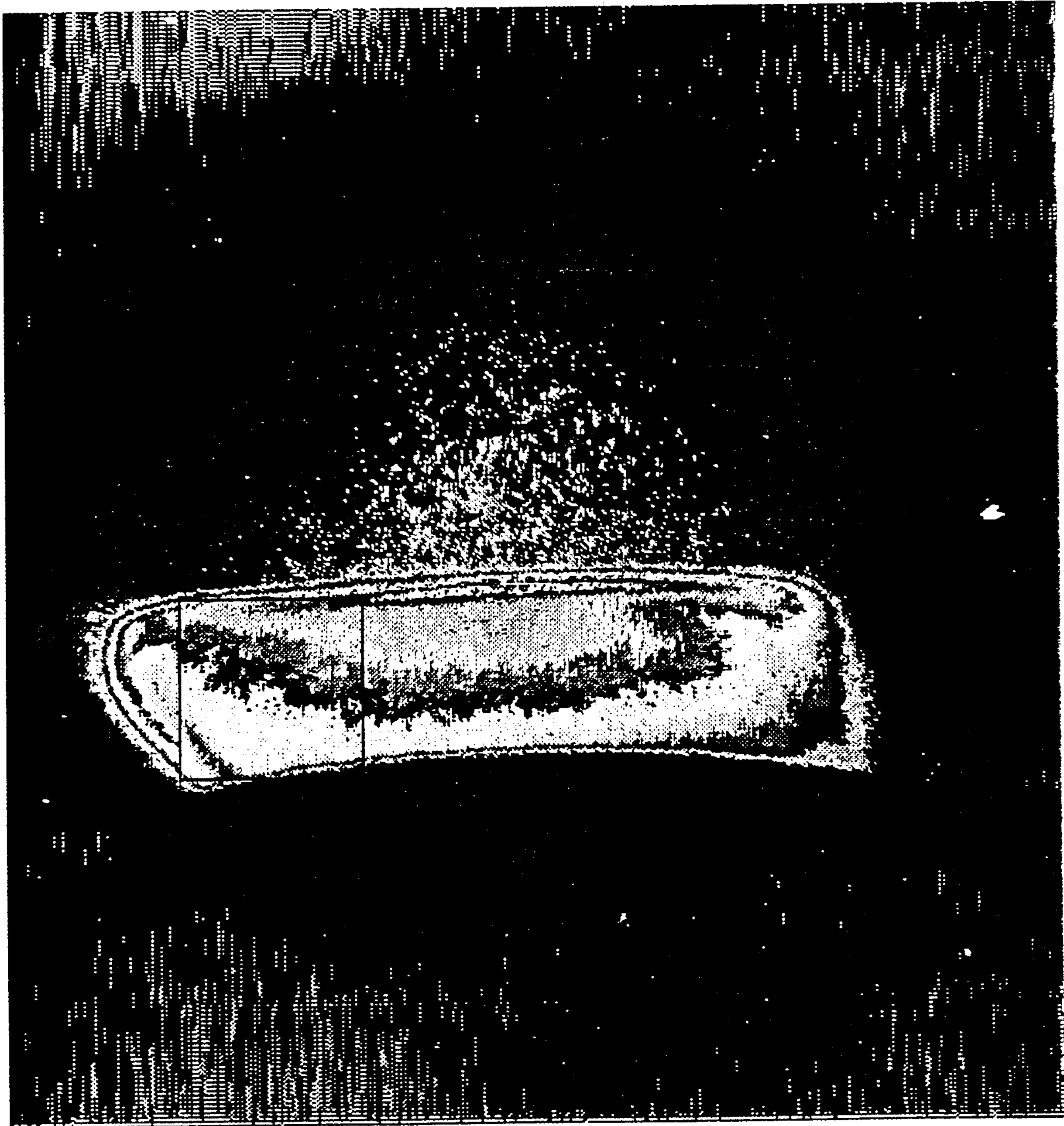

INP-0170

BRAGG-PEAK-SHIFT	BRAGG-PEAK-BROADENING	INTEGRATED-INTENSITY
	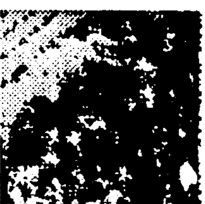	
MAX= 30.260 DEG	MAX= 0.10000	MAX= 56.0000
AVG= 30.1600 DEG	AVG= 0.06000	AVG= 39.0000
MIN= 30.0000 DEG	MIN= 0.00083	MIN= 4.0000

BRIMROSE D A R C X-RAY TOPOGRAPHY SYSTEM

DIGITAL AUTOMATED ROCKING CURVE TOPOGRAPHY

PRINT 2B

PRINT 3A

PRINT 3B

WACKER GAAS-A 66.2/.75DEG (400) 11/17/87 11:37

BRAGG-PEAK-SHIFT	BRAGG-PEAK-BROADENING	INTEGRATED-INTENSITY
		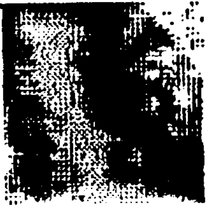
MAX= 33.222 DEG	MAX= 0.03740	MAX= 60.0000
AVG= 33.1841 DEG	AVG= 0.01870	AVG= 47.0000
MIN= 33.1000 DEG	MIN= 0.00000	MIN= 3.0000

BRIMROSE D A R C X-RAY TOPOGRAPHY SYSTEM

DIGITAL AUTOMATED ROCKING CURVE TOPOGRAPHY

PRINT 3C

WACKER GAAS-A 66.2/.75DEG (400) 11/17/87 11:37

BRAGG-PEAK-SHIFT   BRAGG-PEAK-BROADENING   INTEGRATED-INTENSITY

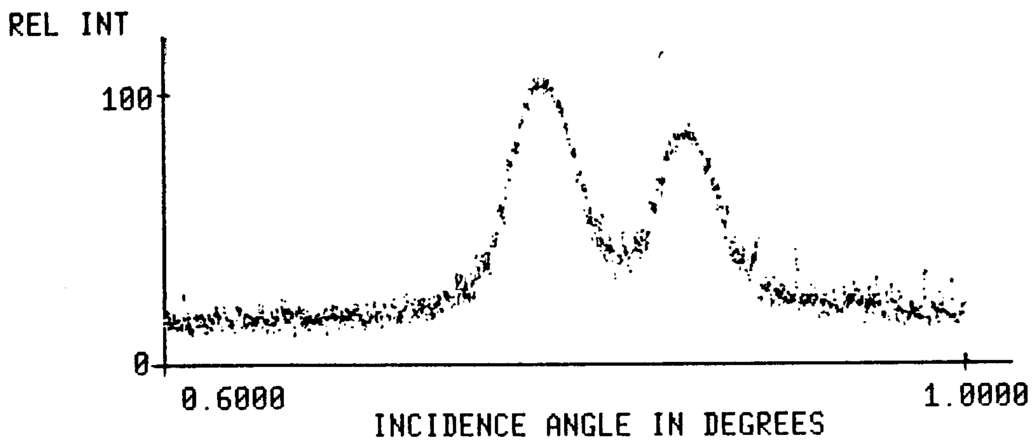

BRIMROSE D A R C X-RAY TOPOGRAPHY SYSTEM

DIGITAL AUTOMATED ROCKING CURVE TOPOGRAPHY

PRINT 3D